Consistent with the characteristics of most types of connective tissue, cell turnover within the disc is slow. Moreover, progenitor cells are present in the disc, which, on activation, could replace resident cells (10). Thus, tissue renewal in the intervertebral disc is dependent on the ability of progenitor cells to commit to the annulus fibrosus/nucleus pulposus lineage and undergo terminal differentiation. These events become even more important during disc degeneration and aging, since the number of cells in the annulus and nucleus pulposus decrease as a result of apoptosis and senescence (11–13).

Proliferation of progenitor cells is regulated by the hypoxia-sensitive Notch signaling pathway (14). Interaction between HIF-1α and the intracellular domain of the Notch protein (Notch-ICD) inhibits differentiation of myogenic and neural precursor cells (15). In skeletal tissue, disruption of Notch signaling markedly increases trabecular bone mass; indeed, mouse studies have shown that, with aging, osteopenia develops, due to a sharp reduction in mesenchymal progenitor cell populations in the mice (16,17). In articular cartilage, Notch signaling maintains the proliferation of chondrocytes, while during cell differentiation, there is a decrease in Notch signaling as well as a decrease in the expression of the target gene Hes5 (18). Hypoxia also increases the expression of known Notch target genes, such as Hes1 and Hey1 (15). Accordingly, in the nucleus, HIF-1α may directly interact with the Notch-ICD and direct cell fate.

The major objective of the present investigation was to examine the hypothesis that hypoxia regulates Notch signaling activity in intervertebral disc cells, and that this pathway is critical for the maintenance of cell proliferation. Our results show, for the first time, that in disc cells, hypoxia serves as a positive modulator of Notch signaling and Hes1 expression.

MATERIALS AND METHODS

Reagents and plasmids. Plasmids were kindly provided by Dr. Urban Lendahl (Karolinska Institute, Stockholm, Sweden) (plasmids 12xCSL-Luc and Hes1-Luc [−194/+160 bp]) (15) and Dr. Diane Hayward (Johns Hopkins University, Baltimore, MD) (plasmids 4xwtCBF1-Luc and 4xmtCBF1-Luc). Notch1-ICD, developed by Dr. Conie Cepko (Harvard Medical School, Department of Genetics, Boston, MA), was obtained from Addgene (no. 15131) (19). As an internal transfection control, vector pRL-TK (Promega), containing the *Renilla reniformis* luciferase gene, was used. The amount of transfected plasmid, the pretransfection period after seeding, and the posttransfection period before harvesting have been optimized for rat nucleus pulposus cells using pSV β-galactosidase plasmid (Promega) (9). The γ-secretase/Notch signaling inhibitor L685458 was from Sigma.

Isolation of rat intervertebral disc cells, and culture of cells in a state of hypoxia. Nucleus pulposus and inner annulus fibrosus cells were isolated from rat lumbar discs (obtained from 10–12-week-old rats), using a method previously described by Risbud et al (9). Cells were maintained in Dulbecco's modified Eagle's medium (DMEM) and 10% fetal bovine serum (FBS) supplemented with antibiotics. Both inner annulus fibrosus cells and nucleus pulposus cells were cultured in a Hypoxia Work Station (Invivo$_2$ 300) with a mixture of 1% O_2, 5% CO_2, and 94% N_2 for 24–72 hours. The concentration of oxygen chosen for this study was based on our previous observations from in vitro studies, as well as on information generated on the oxemic status of the disc in vivo.

Collection and grading of human tissue. Lumbar disc tissue samples were collected as surgical waste from individuals undergoing elective spinal surgical procedures (mean age 54 years, range 38–82 years). Control samples from cadaver donors were obtained from regional tissue banks. In accordance with the guidelines of the Thomas Jefferson University Institutional Review Board, informed consent for sample collection was obtained from each patient. Assessment of intervertebral disc disease was performed using the modified Thompson grading system (20).

Immunohistologic studies. Freshly isolated rat spines were immediately fixed in 4% paraformaldehyde in phosphate buffered saline (PBS) and then embedded in paraffin. Transverse sections, 6–8 μm in thickness, were deparaffinized in xylene and rehydrated through graded ethanol. For localization of Notch-4 protein in the tissue, sections were incubated with anti–Notch-4 antibodies (1:150) in 2% bovine serum albumin in PBS, at a dilution of 1:100, at 4°C overnight. After thoroughly washing the sections, the bound primary antibody was incubated with a biotinylated universal secondary antibody (Vector), at a dilution of 1:20, for 10 minutes at room temperature. Sections were incubated with a streptavidin–peroxidase complex for 5 minutes and washed with PBS. The color reaction was developed using 3,3′-diaminobenzidine (Vectastain Universal Quick Kit; Vector).

Real-time reverse transcription–polymerase chain reaction (RT-PCR) analysis. Total RNA was extracted from rat annulus fibrosus and nucleus pulposus cells or tissue sections using RNeasy Mini columns (Qiagen). Before elution from the column, RNA was treated with RNase-free DNase I (Qiagen). In human tissue samples, total RNA was isolated from 100–300 mg of disc tissue. The tissue was homogenized in Trizol (Invitrogen) on ice, using an Omni TH Homogenizer (Omni International). Following extraction with TRIzol, RNA was passed through the RNeasy Mini columns. The purified, DNA-free RNA was converted to complementary DNA (cDNA) using Superscript III Reverse Transcriptase (Invitrogen).

Reactions were set up in triplicate in 96-well plates, using 1 μl cDNA with SYBR Green PCR Master Mix (Applied Biosystems), to which gene-specific forward and reverse PCR primers were added (synthesized by Integrated DNA Technologies). PCR reactions were performed in a StepOnePlus real-time PCR system (Applied Biosystems), in accordance with the manufacturer's instructions; expression values were normalized to those of 18S cDNA and GAPDH. Melting curves were analyzed to verify the specificity of the RT-PCR and the absence of primer dimer formation.

Protein extraction and Western blotting. Rat disc cells were placed on ice immediately following treatment, and then washed with ice-cold Hanks' balanced salt solution. All of the wash buffers and the final resuspension buffer included 1X protease inhibitor cocktail (Roche), NaF (5 m*M*), and Na_3VO_4 (200 μM). Nuclear or total cell proteins were resolved on 8–12% sodium dodecyl sulfate–polyacrylamide gels and transferred by electroblotting to PVDF membranes (Bio-Rad). The membranes were blocked with 5% nonfat dry milk in TBST (50 m*M* Tris, pH 7.6, 150 m*M* NaCl, 0.1% Tween 20) and incubated overnight at 4°C in 3% nonfat dry milk in TBST with anti–Notch-4 antibodies (1:600; Santa Cruz Biotechnology), anti–Jagged-1 antibodies (1:1,000; Cell Signaling Technology), anti-Hes1 antibodies (1:500; Santa Cruz Biotechnology), or anti–β-tubulin antibodies (1:2,000; Developmental Studies Hybridoma Bank). Immunolabeling was detected using an enhanced chemiluminescence reagent (Amersham Biosciences).

Immunofluorescence microscopy. Rat disc cells were plated in flat-bottomed 96-well plates (5×10^3/well) and cultured under hypoxic conditions for 24 hours. After incubation, cells were fixed with 4% paraformaldehyde, permeabilized with 0.2% Triton X-100 in PBS for 10 minutes, blocked with PBS containing 5% FBS, and incubated with antibodies against cleaved Notch1 (1:200; Cell Signaling Technology), Notch3 (1:200), Notch4 (1:100), or Hes1 (1:100) (the latter 3 from Neuromics), at 4°C overnight. As a negative control, cells were reacted with isotype IgG under similar conditions. After washing, the cells were incubated with an Alexa Fluor 488–conjugated anti-mouse secondary antibody (Invitrogen), at a dilution of 1:50, for 1 hour at room temperature. Cells were imaged using a laser scanning confocal microscope (Olympus Fluoview).

Transfections and dual luciferase assay. Rat disc cells were transferred, one day before transfection, to 24-well plates at a density of 4×10^4 cells/well. To investigate the effect of Notch-ICD overexpression on CBF1 and Hes1 promoter activity, cells were cotransfected with Notch-ICD (100–300 ng), or appropriate backbone vector, along with 300–350 ng CBF1 or Hes1 reporter and 300–350 ng pRL-TK plasmid. To measure the effect of hypoxia on Notch signaling, cells were transfected with 500 ng of 12xCSL or CBF1 reporter plasmids along with 500 ng pRL-TK plasmid; in some experiments, cells were treated with the Notch inhibitor L685458 (4 μM; Sigma). Lipofectamine 2000 (Invitrogen) was used as a transfection reagent. For each transfection, plasmids were premixed with the transfection reagent.

Within 48–72 hours after transfection, the cells were harvested and a dual luciferase reporter assay system (Promega) was used for sequential measurements of firefly and *Renilla* luciferase activities. Quantification of the luciferase activities and calculation of relative expression ratios were carried out using a luminometer (TD-20/20; Turner Designs). At least 3 independent transfections were performed, and all analyses were carried out in triplicate.

Assessment of cell proliferation by MTT assay. To measure disc cell proliferation, an MTT assay was carried out as described previously (5). Briefly, after treatment of the rat disc cells, MTT diluted in serum-free DMEM was added to the culture medium, to a final concentration of 0.5 mg/ml. At the end of the incubation period (2 hours at 37°C), the medium was removed, and the precipitated formazan crystals were solubilized in dimethyl sulfoxide. Product formation was measured by reading the absorbance at 560 nm, using a microplate reader (Tecan; Spectra Flour Plus).

Analysis of cell cycle. Following treatment of the rat annulus fibrosus cells, a single-cell suspension was prepared from cell cultures and fixed in ice-cold 70% ethanol for 1 hour. Cells were washed and resuspended in PBS with 5% FBS, and then incubated with 50 μM propidium iodide for 30 minutes at 37°C. Analysis of the cell cycle was conducted using a Coulter Epics XL-MCL system, with results analyzed using the XL System II software.

Statistical analysis. All measurements were performed in triplicate. Results are presented as the mean ± SEM. Differences between groups were assessed by analysis of variance. P values less than 0.05 were considered statistically significant.

RESULTS

Transverse sections of skeletally mature rat discs were stained with antibodies to Notch-4 (Figure 1A). Notch-4 was observed to be present in cells of the annulus fibrosus and nucleus pulposus. Staining was evident in the plasma membrane and cytosol, as well as nucleus (Figure 1A).

Expression of select Notch pathway proteins in the rat disc tissue was studied using Western blot analysis. As shown in Figure 1B, the rat nucleus pulposus and annulus fibrosus tissue expressed Notch-4, Jagged-1, and Notch target gene Hes1. Expression of Hes1 was most prominent in the nucleus pulposus (Figure 1B), while that of Jagged-1 was higher in the annulus fibrosus.

To further examine the expression of different Notch receptors and ligands in the disc tissue, messenger RNA (mRNA) expression in the annulus fibrosus tissue was analyzed by RT-PCR (Figure 1C). We observed expression of mRNA for the Notch ligands Jagged1, Jagged2, and Delta1 and Notch receptors 1–4. However, expression of Delta3 was undetectable. Nucleus pulposus tissue elicited a similar pattern of ligand and receptor mRNA expression (results not shown).

In parallel, we measured the relative mRNA expression of Notch receptors in primary cells of the annulus fibrosus and nucleus pulposus. As shown in Figures 1D and E, a raised expression of Notch2, when compared with the other receptors, was observed in both cell types. Moreover, in annulus fibrosus cells, expression of Notch3 was higher than that of Notch1 and Notch4. Immunofluorescence analysis confirmed that Notch1, Notch3, and Notch4, as well as Jagged1, were

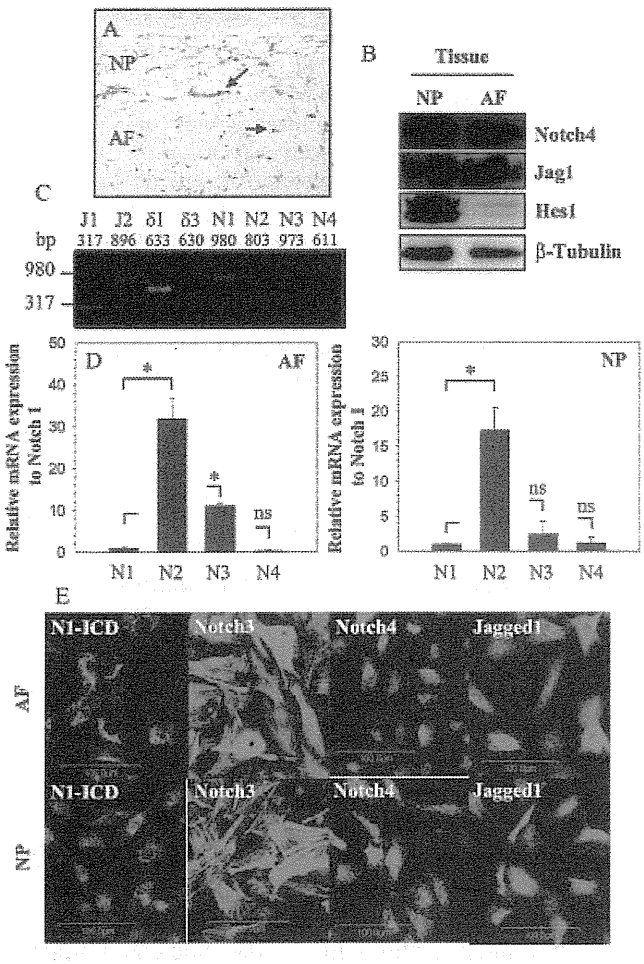

Figure 1. Expression of Notch receptors and ligands, as well as Notch target gene Hes1, in rat intervertebral discs. **A,** Transverse sections of disc tissue from mature rats were treated with anti–Notch-4 antibodies, and expression of Notch-4 was detected in cells of the nucleus pulposus (**NP**) and annulus fibrosus (**AF**) (**arrows**). Original magnification × 20. **B,** Expression of Notch-4, Jagged-1, and Hes1 was assessed in NP and AF tissue by Western blotting; anti–β-tubulin was used as a positive control. **C,** Expression of select Notch ligands (Jagged1 [J1], Jagged2 [J2], Delta1, and Delta3) and Notch receptors (N1–N4) was assessed in AF tissue by reverse transcription–polymerase chain reaction (RT-PCR). **D,** Messenger RNA expression of the 4 Notch receptors was assessed in primary cells of the AF (left) and NP (right) by real-time RT-PCR. Values for Notch2–Notch4 are expressed relative to that of Notch1 and are the mean ± SEM results from 3 independent experiments. * = $P < 0.05$. NS = not significant. **E,** AF and NP cells were assessed by immunofluorescence analysis for the expression of Notch3, Notch4, and Jagged1, as well as cleaved Notch1 (Notch1–intracellular domain [N1-ICD]). Original magnification × 20.

expressed in annulus fibrosus and nucleus pulposus cells (Figure 1F).

We also examined the relationship between expression of Notch receptors in disc cells and the oxemic status of the cells. As shown in Figure 2A, when annulus fibrosus and nucleus pulposus cells were cultured under conditions of hypoxia for 8 hours, Notch1 mRNA was induced. In contrast, Notch2 mRNA expression was elevated with hypoxia in nucleus pulposus cells only (Figure 2B). With regard to Notch3 mRNA, expression

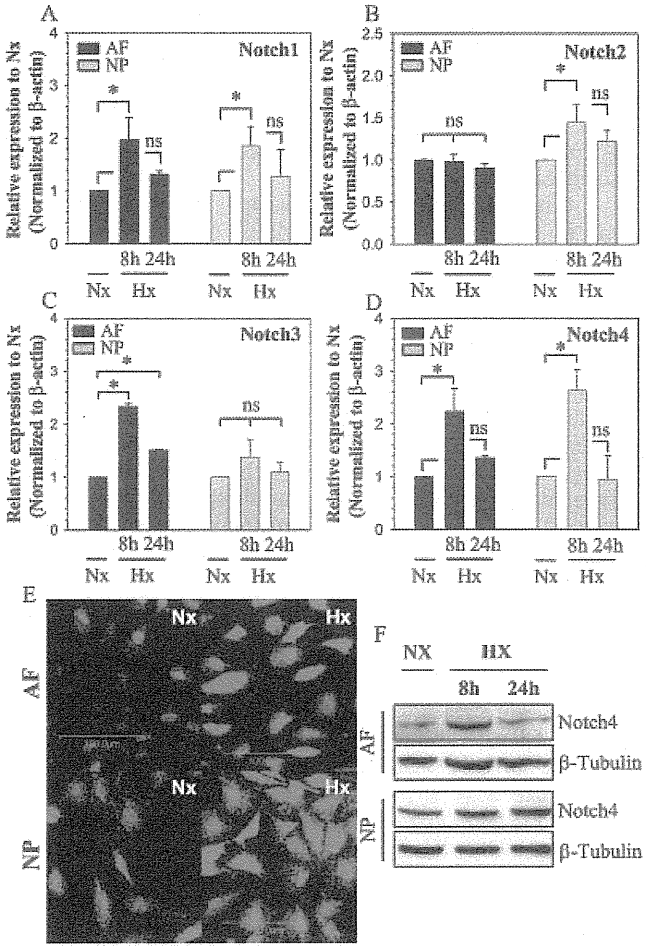

Figure 2. Hypoxic regulation of Notch receptor expression in rat disc cells. **A–D,** AF and NP cells were cultured under conditions of hypoxia (Hx) for 8 or 24 hours, or under normoxic (Nx) conditions, and the response to hypoxia was assessed by real-time reverse transcription–polymerase chain reaction analysis of mRNA expression for Notch receptors Notch1 (**A**), Notch2 (**B**), Notch3 (**C**), and Notch4 (**D**). Values are the mean ± SEM results from 3 independent experiments. * = $P < 0.05$. **E** and **F,** Notch-4 protein expression under conditions of hypoxia, or under normoxic conditions, was assessed in AF and NP cells by immunofluorescence analysis (after 24 hours of hypoxia) (**E**) and Western blotting (after 8 and 24 hours of hypoxia) (**F**). Anti–β-tubulin was used as a positive control in Western blots. Original magnification × 20. See Figure 1 for other definitions.

was induced by hypoxia in annulus fibrosus cells but not in nucleus pulposus cells (Figure 2C). Finally, expression of Notch4 mRNA was induced by hypoxia in both cell types (Figure 2D).

To determine whether there was a concomitant elevation in Notch-4 protein expression associated with the oxemic status, the cells were evaluated by immunofluorescence analysis and Western blotting. In both cell types, there was an increase in Notch-4 expression in the hypoxic cultures, as indicated in Figures 2E and F. Protein expression was maximally elevated at 8 hours and returned to baseline levels by 24 hours in annulus fibrosus cells, while in nucleus pulposus cells, protein expression remained elevated up to 24 hours.

We then examined the effect of hypoxia on mRNA expression of the Notch ligands Jagged1 and Jagged2 in disc cells. As shown in Figure 3A, under conditions of hypoxia, there was induction of Jagged1 mRNA in annulus cells but not in nucleus pulposus cells. In contrast, in both annulus fibrosus and nucleus pulposus cells, Jagged2 mRNA expression was highly sensitive to hypoxia (Figure 3B). In both cell types, mRNA expression remained elevated for the first 8 hours; in annulus fibrosus cells, mRNA expression returned to baseline levels by 24 hours. In addition, the effect of hypoxia on Jagged-1 protein expression was examined in annulus fibrosus cells by Western blotting (Figure 3C) and immunofluorescence microscopic analysis (Figure 3D). In the hypoxic environment, a significant increase in the levels of Jagged-1 protein was seen (Figures 3C and D).

To further evaluate the relationship between Notch signaling and oxygen tension, we measured the expression of Notch target gene Hes1 in the rat disc cells under normoxic and hypoxic conditions. In annulus fibrosus cells, expression of Hes1 mRNA was induced after 8 hours of hypoxia and returned to baseline levels by 24 hours (Figure 3E). In contrast, in nucleus pulposus cells, Hes1 mRNA expression was insensitive to hypoxia. Western blot analysis showed that Hes-1 protein expression was also elevated in hypoxia, and stayed high in annulus fibrosus cells under hypoxic conditions for 24 hours (Figure 3F). As expected, Hes-1 protein expression in nucleus pulposus cells remained unchanged (Figure 3F).

To investigate whether Hes1 responds to Notch signaling, we cotransfected annulus fibrosus cells with a Notch-ICD expression plasmid, and then measured Hes1 promoter activity. Induced overexpression of Notch resulted in increased Hes1 promoter activity

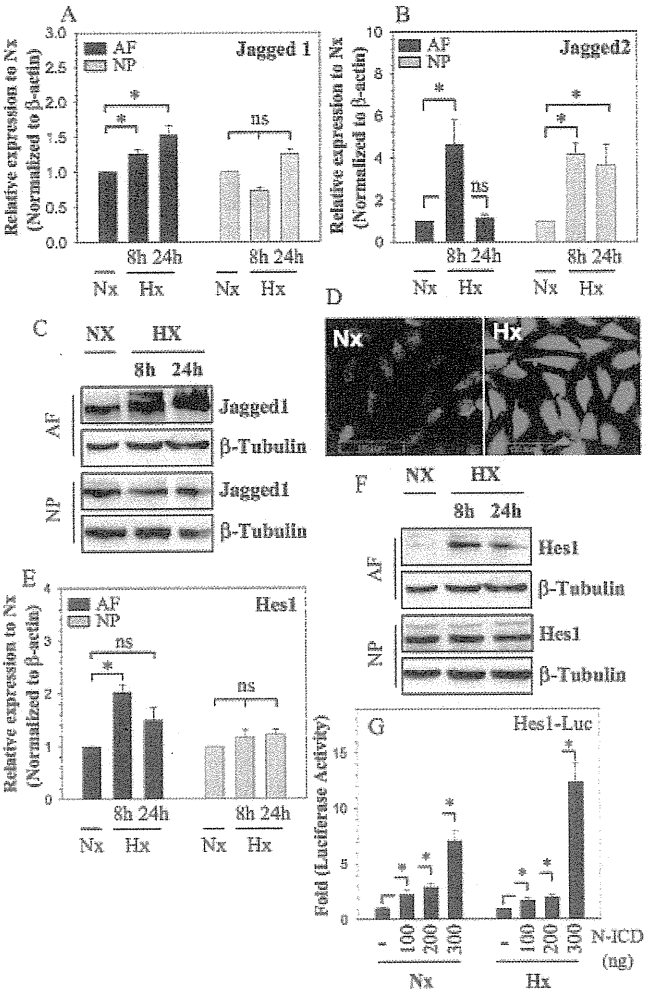

Figure 3. Hypoxic regulation of Notch ligand expression in rat disc cells. **A** and **B,** AF and NP cells were cultured under conditions of hypoxia (Hx) for 8 or 24 hours, or under normoxic conditions (Nx), and the response to hypoxia was assessed by real-time RT-PCR analysis of Jagged1 (**A**) and Jagged2 (**B**) mRNA expression. **C** and **D,** Jagged-1 protein expression under conditions of hypoxia, or under normoxic conditions, was assessed in AF and NP cells by Western blotting (after 8 and 24 hours) (**C**) and immunofluorescence analysis (after 24 hours) (**D**). Anti–β-tubulin was used as a positive control in Western blots. Original magnification × 20. **E** and **F,** The effect of hypoxia on Hes1 gene expression and promoter activity was assessed in AF and NP cells cultured for 8 or 24 hours under conditions of hypoxia, or under normoxic conditions, using real-time RT-PCR analysis of Hes1 mRNA expression (**E**) and Western blotting of Hes-1 protein expression, with anti–β-tubulin used as a positive control (**F**). **G,** AF cells were cotransfected with a Hes1 reporter (−194/+160 bp) along with increasing doses of Notch1–intracellular domain (N-ICD), and Hes1 reporter activity was measured under normoxic and hypoxic conditions. Values in **A, B, E,** and **G** are the mean ± SEM results from 3 independent experiments. * = $P < 0.05$. See Figure 1 for other definitions.

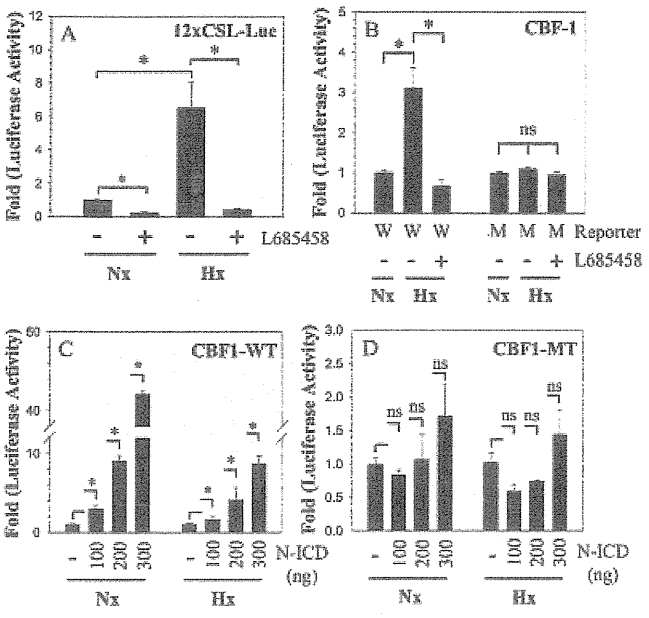

Figure 4. Effect of hypoxia on Notch signaling activity. **A** and **B,** The 12xCSL reporter **(A)** or CBF1 reporter containing a wild-type (W) or mutant (M) RBPJκ motif **(B)** was transfected into rat annulus fibrosus cells along with pRL-TK vector. Cells were cultured for 24 hours under normoxic conditions (21% O_2) (Nx) or hypoxic conditions (1% O_2) (Hx), and some cells were treated with γ-secretase inhibitor L685458 (4 μM), and luciferase reporter activity was measured. **C** and **D,** Rat annulus fibrosus cells were cotransfected with wild-type (WT) **(C)** or mutant (MT) **(D)** CBF1 reporters along with increasing doses of Notch1-ICD, and reporter activity was measured under normoxic and hypoxic conditions. Values are the mean ± SEM results from 3 independent experiments. $* = P < 0.05$. See Figure 1 for other definitions.

under conditions of normoxia, and led to an even greater level of Hes1 promoter activity in the hypoxic state (Figure 3G).

We next evaluated the effect of hypoxia on the activity of the Notch-responsive reporter 12xCSL and Notch target gene CBF1 in annulus fibrosus cells (Figures 4A and B). Hypoxia significantly induced 12xCSL reporter activity. Moreover, induction of reporter activity was completely blocked by the γ-secretase inhibitor L685458. Similarly, hypoxia increased CBF1 promoter activity, and this was also significantly blocked by inhibitor treatment.

A CBF1 promoter harboring a mutation in the Notch-interacting RBPJκ site is insensitive to both hypoxia and L685458 treatment. To further validate that CBF1 promoter activity is responsive to Notch signaling, we cotransfected annulus fibrosus cells with a plasmid encoding the Notch1-ICD. This plasmid significantly increased wild-type CBF1 promoter activity, under both normoxic and hypoxic conditions (Figure 4C). The stimulatory effect of Notch-ICD on CBF1 promoter activity was evident in cultures with 100 ng of plasmid, and the effect was further enhanced when the concentration of plasmid was increased to 300 ng (Figure 4C). Moreover, the inductive effect was more pronounced in a state of normoxia. As expected, mutant CBF1 promoter activity was unresponsive to Notch coexpression (Figure 4D).

We also examined the relationship between Notch signaling and proliferation of annulus fibrosus cells. Treatment with γ-secretase inhibitor L685458 re-

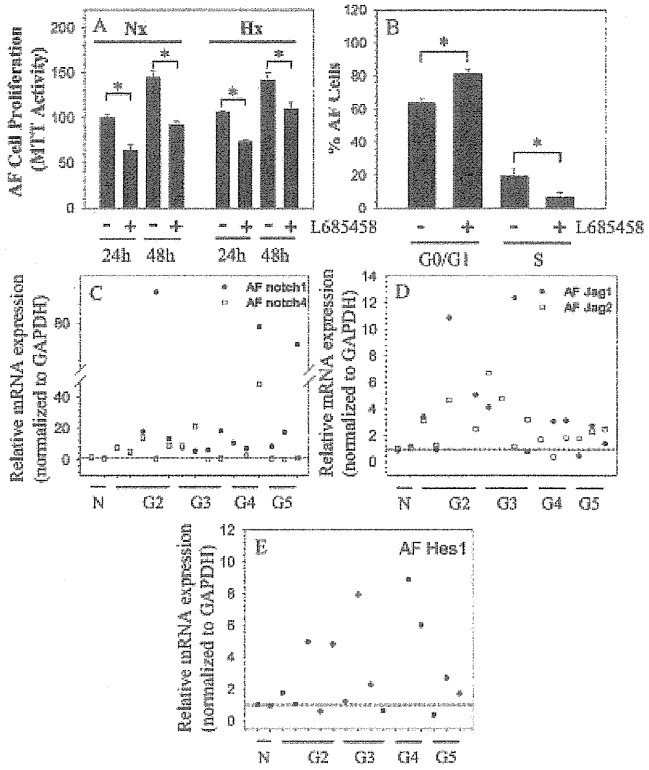

Figure 5. Role of Notch signaling in controlling AF cell proliferation. **A,** AF cells were cultured under normoxia (Nx) or hypoxia (Hx), with or without γ-secretase inhibitor L685458 (4 μM), for 24–48 hours, and cell proliferation was measured by MTT assay. **B,** The cell cycle of AF cells treated with or without L685458 was determined by flow cytometry, with results expressed as the percentage of AF cells in G0/G1 phase or S phase. Values in **A** and **B** are the mean ± SEM results from 3 independent experiments. $* = P < 0.05$. **C–E,** Messenger RNA expression of Notch receptors Notch1 and Notch4 **(C)**, Notch ligands Jagged1 and Jagged2 **(D)**, and Notch target gene Hes1 **(E)** was assessed by real-time RT-PCR in multiple human AF tissue samples in varying degrees of degeneration (Thompson grades 2–5 [G2–G5]) compared with normal controls (N) (controls n = 2, G2 n = 5, G3 n = 4, G4 n = 3, G5 n = 3). The mean expression of mRNA in normal control samples was set at 1.0 (horizontal line). See Figure 1 for other definitions.

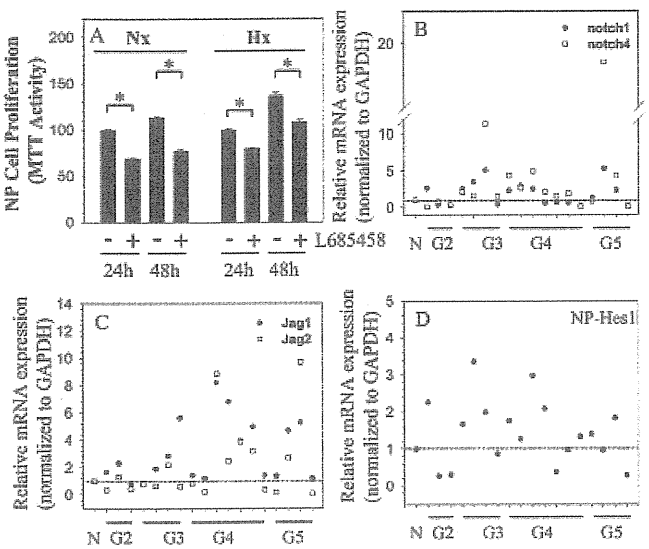

Figure 6. Role of Notch signaling in controlling NP cell proliferation. **A,** NP cells were cultured under conditions of normoxia (Nx) or hypoxia (Hx), with or without γ-secretase inhibitor L685458 (4 μM), for 24–48 hours, and cell proliferation was measured by MTT assay. Values are the mean ± SEM results from 3 independent experiments. * = $P < 0.05$. **B–D,** Messenger RNA expression of Notch receptors Notch1 and Notch4 **(B)**, Notch ligands Jagged1 and Jagged2 **(C)**, and Notch target gene Hes1 **(D)** was assessed by real-time RT-PCR in multiple human NP tissue samples in varying degrees of degeneration (Thompson grades 2–5 [G2–G5]) compared with normal controls (N) (controls n = 1, G2 n = 3, G3 n = 4, G4 n = 7, G5 n = 4). The mean expression of mRNA in normal control samples was set at 1.0 (horizontal line). See Figure 1 for other definitions.

sulted in a significant suppression of annulus fibrosus cell proliferation under both normoxic and hypoxic conditions (Figure 5A). With the use of flow cytometry, we determined whether the cell cycle status was affected by L685458 treatment. The number of annulus fibrosus cells in S phase was significantly decreased after treatment with the inhibitor (mean ± SEM 6.7 ± 2.8%) when compared to the number of untreated control cells in S phase (mean ± SEM 19.25 ± 4.4%) (Figure 5B). In contrast, there was a greater accumulation of cells in G0/G1 phase after treatment (mean ± SEM 81.10 ± 3.3%) as compared to control cells left untreated (mean ± SEM 63.4 ± 2.9% in G0/G1 phase).

Finally, we evaluated the expression of select Notch receptors, ligands, and the target gene Hes1 in Thompson-graded degenerated human annulus fibrosus tissue (Figures 5C–E). Results of real-time RT-PCR analysis showed that there was a trend toward an increase in expression of Notch1 and Notch4 mRNA (Figure 5C) in degenerated human disc tissue when compared to normal controls. Similarly, both Jagged1 and Jagged2 mRNA exhibited a similar trend in expression in degenerated disc tissue (Figure 5D). Hes1 mRNA expression was also responsive to degeneration, as indicated by a higher mRNA expression level at the earlier Thompson stages (grade 2 and grade 3) (Figure 5E). Not surprisingly, there was a considerable between-patient variation within the same grade.

We also examined the role of Notch signaling in regulating proliferation of nucleus pulposus cells. Similar to the effects on annulus fibrosus cells and irrespective of the oxemic tension, L685458 treatment resulted in a significant inhibition of the proliferation of nucleus pulposus cells (Figure 6A).

Finally, we measured the expression of Notch receptors, ligands, and Hes1 in graded degenerated human disc tissue from the nucleus pulposus (Figures 6B–D). Results of real-time RT-PCR analysis showed that there was a trend toward an increase in mRNA expression of Notch1 and Notch4 (Figure 6B) and Jagged1 and Jagged2 (Figure 6C) in degenerated human disc tissue when compared to normal controls. Similarly, there was a trend toward an increase in the expression of Hes1 mRNA in the degenerated nucleus pulposus (Figure 6D). As in the degenerated tissue of the annulus fibrosus, a considerable between-patient variation in mRNA expression was observed in the degenerated nucleus pulposus, among tissue of the same Thompson grade.

DISCUSSION

The basis for the studies described herein is that progenitor cell populations are present in the hypoxic tissue of the intervertebral disc (10). Accordingly, it would not be unreasonable to assume that the commitment of these cells into functioning cells of the annulus fibrosus and nucleus pulposus is dependent on the highly conserved, hypoxia-sensitive Notch signaling pathway (14,15,21). The present study revealed that there is a hypoxia-dependent increase in expression of specific Notch ligands and receptors and a concomitant increase in Notch signaling activity. In addition, we found that hypoxia induces expression of Hes1, the Notch target gene that is associated with maintenance of the undifferentiated state and determination of cell fate (22,23).

Accordingly, as has also been observed in articular cartilage, the hypoxic status of the disc may serve to conserve cell number and maintain the differentiated state of the cells by regulating Notch signaling activity (18). Our results showed that there is an increase in levels of Notch signaling proteins in degenerated human

disc tissue; however, the response is probably insufficient to maintain cell numbers and preserve the differentiated state of the cells. This observation could explain why there is a gradual age-dependent loss of cells and a decrease in the ability of resident cells to mount a reparative response.

In this study, we examined the expression and localization of Notch receptors and ligands in the intervertebral disc of skeletally mature animals. Both annulus fibrosus and nucleus pulposus tissue expressed Notch receptors (Notch-1–Notch-4) and ligands (Jagged-1, Jagged-2, and Delta-1). The observation that there was robust expression of the Notch target gene, Hes1, indicated the presence of an active Notch signaling pathway in the disc, a notion supported by the plethora of receptors and ligands that were present in both tissue types; a similar spectrum of receptors and ligands has been observed in cartilage (24). Consistent with this observation, although the study focused on defining components of the signaling pathway in specific tissues of the intervertebral disc, it would not be surprising to find that ligands from the inner annulus are associated with Notch receptors in the nucleus pulposus; likewise, ligands in the nucleus would serve to activate Notch signaling pathways in the annulus fibrosus. This interaction would be consistent with the notion that the disc itself represents an environmental niche that serves to integrate the functional activities of each of the component tissues (1).

There were marked differences in the pattern of expression of Notch receptors and ligands in the disc. While Notch2 mRNA transcript levels were elevated in both the annulus and the nucleus pulposus, Jagged-1 protein levels were significantly greater in the annulus than in the nucleus pulposus. In both tissues, Notch1 and Notch4 reporter expression was responsive to the level of Po_2. In nucleus cells, Notch reporter expression was increased with hypoxia.

To examine the premise that hypoxia influences Notch signaling activity, the Notch-responsive reporters 12xCSL and CBF1 were utilized. Our results showed that there was increased activity of both reporters under hypoxic conditions. Moreover, reporter activity was completely inhibited when the hypoxic cells were treated with the γ-secretase inhibitor L685458. We confirmed the involvement of the signaling pathway using a reporter with a mutation in the CSL-binding site. In this case, hypoxic induction of Notch reporter activity was completely blocked. Results of these experiments lend direct support to the hypothesis that hypoxia promotes Notch signaling in disc cells. This result is consistent with observations of activation of Notch signaling in stem cells and other cell types (16,17) and confirms previous findings showing that the Notch signaling pathway is responsive to hypoxia (14,15,21). Of note, since disc cells function in vivo in a low oxemic environment, it is likely that hypoxia is a key factor regulating the activity of this pathway (14,15,21,25).

In addition to the effects of hypoxia on Notch ligands and receptors, we noted that there was a hypoxia-dependent increase in Notch target gene activity. This finding suggests that in disc cells, Hes1 expression is regulated in a hypoxia-dependent manner. It should be noted that in many types of tissue, Hes1 is considered to be a key regulator of differentiation (23,26). Hes1 is expressed by almost all undifferentiated cells and is required for the maintenance of this pool of cells. The observation that a progenitor cell pool is present in the disc, even in degenerated disc tissue (10), adds credence to the view that the hypoxic state enhances the activity of this powerful repressor of differentiation (23,26). Not surprisingly, the response of disc cells to HIF is markedly different from that of myogenic C2C12 cells (7,9,27). In stem cells and many cancer cells, HIF-1 interacts with the Notch coactivator Mastermindlike-1 to increase Hes-1 promoter activity (25). Possibly, in the disc, HIF-1α may promote recruitment of the Notch-ICD to the CSL-binding motifs in the Hes1 promoter (15). While the mechanism by which this type of regulation is achieved is still under examination, functionally, it is more than likely a reflection of the normative environment of hypoxia in the disc.

Although regulation of Notch activity may be tissue specific, the signaling pathway has been shown to modulate cell proliferation and differentiation, as well as self renewal (18,22,23,26). To determine whether the Notch pathway regulates disc cell number, we evaluated nucleus pulposus and annulus fibrosus cell proliferation under normoxic and hypoxic conditions. In both cases, when treated with a γ-secretase inhibitor, a marked decrease in proliferation was observed. We reasoned that this suppressive effect would account for the decrease in cell number that characterizes degenerated human disc tissue (11–13).

Based on this observation, we evaluated major components of the Notch signaling pathway in cells of human discs in varying degrees of degeneration. While the number of control tissue samples was very limited (due to practical difficulties in acquiring normal human discs), measurement of mRNA expression levels suggested that as the tissue became degenerated, there was a rise in expression of Jagged1 and Jagged2 and possibly Notch4 and Hes1. Our results are consistent with those of a recent study that showed increased expression of

Notch1, Jagged1, and Hes5 in osteoarthritic cartilage (28). One explanation for the increase is that it possibly represents a compensatory response by resident cells to replace the lost or nonfunctional cells. Indeed, in the disc, as well as cartilage, a clonal proliferative response is a hallmark of degeneration (29–31). In both tissues, aside from the effects of hypoxia, other regulatory elements, including elevated signaling through the transforming growth factor β/Smad3 and Wnt/β-catenin pathways, are likely to modulate Notch pathway activity (32–35). Thus, although some increase in the levels of Notch signaling proteins may occur, the dysregulated response is insufficient to mount a complete functional recovery and restoration of cell numbers in the tissue.

In terms of pursuing therapeutic strategies, it should be possible to promote tissue repair by 3 different approaches. First, specific ligands and receptors of the Notch signaling pathway may be manipulated to reactivate the surviving endogenous progenitor cells to promote their proliferation and subsequent commitment to the annulus fibrosus and nucleus pulposus cell phenotype. Second, molecules, such as the numb protein, that antagonize Notch signaling activity may be targeted in disc progenitor cells (36). Finally, the oxemic status of the intervertebral niche may be restored using redox-sensitive agents.

AUTHOR CONTRIBUTIONS

All authors were involved in drafting the article or revising it critically for important intellectual content, and all authors approved the final version to be published. Dr. Risbud had full access to all of the data in the study and takes responsibility for the integrity of the data and the accuracy of the data analysis.

Study conception and design. Anderson, Sakai, Mochida, Albert, Shapiro, Risbud.

Acquisition of data. Hiyama, Skubutyte, Markova, Anderson, Yadla.

Analysis and interpretation of data. Hiyama, Skubutyte, Markova, Anderson, Yadla, Shapiro, Risbud.

REFERENCES

1. Risbud MV, Schipani E, Shapiro IM. Hypoxic regulation of nucleus pulposus cell survival: from niche to notch. Am J Pathol 2010;176:1577–83.
2. Gruber HE, Ashraf N, Kilburn J, Williams C, Norton HJ, Gordon BE, et al. Vertebral endplate architecture and vascularization: application of micro-computerized tomography, a vascular tracer, and immunocytochemistry in analyses of disc degeneration in the aging sand rat. Spine 2005;30:2593–600.
3. Hassler O. The human intervertebral disc: a micro-angiographical study on its vascular supply at various ages. Acta Orthop Scand 1969;40:765–72.
4. Rudert M, Tillmann B. Lymph and blood supply of the human intervertebral disc: cadaver study of correlations to discitis. Acta Orthop Scand 1993;64:37–40.
5. Bartels EM, Fairbank JC, Winlove CP, Urban JP. Oxygen and lactate concentrations measured in vivo in the intervertebral discs of patients with scoliosis and back pain. Spine 1998;23:1–7.
6. Lee DC, Adams CS, Albert TJ, Shapiro IM, Evans SM, Koch CJ. In situ oxygen utilization in the rat intervertebral disc. J Anat 2007;210:294–303.
7. Rajpurohit R, Risbud MV, Ducheyne P, Vresilovic EJ, Shapiro IM. Phenotypic characteristics of the nucleus pulposus: expression of hypoxia inducing factor-1, glucose transporter-1 and MMP-2. Cell Tissue Res 2002;308:401–7.
8. Agrawal A, Gajghate S, Smith H, Anderson DG, Albert TJ, Shapiro IM, et al. Cited2 modulates hypoxia-inducible factor–dependent expression of vascular endothelial growth factor in nucleus pulposus cells of the rat intervertebral disc. Arthritis Rheum 2008;58:3798–808.
9. Risbud MV, Guttapalli A, Stokes DG, Hawkins D, Danielson KG, Schaer TP, et al. Nucleus pulposus cells express HIF-1α under normoxic culture conditions: a metabolic adaptation to the intervertebral disc microenvironment. J Cell Biochem 2006;98:152–9.
10. Risbud MV, Guttapalli A, Tsai TT, Lee JY, Danielson KG, Vaccaro AR, et al. Evidence for skeletal progenitor cells in the degenerate human intervertebral disc. Spine 2007;32:2537–44.
11. Bertram H, Nerlich A, Omlor G, Geiger F, Zimmermann G, Fellenberg J. Expression of TRAIL and the death receptors DR4 and DR5 correlates with progression of degeneration in human intervertebral disks. Mod Pathol 2009;22:895–905.
12. Tschoeke SK, Hellmuth M, Hostmann A, Robinson Y, Ertel W, Oberholzer A, et al. Apoptosis of human intervertebral discs after trauma compares to degenerated discs involving both receptor-mediated and mitochondrial-dependent pathways. J Orthop Res 2008;26:999–1006.
13. Gruber HE, Ingram JA, Davis DE, Hanley EN Jr. Increased cell senescence is associated with decreased cell proliferation in vivo in the degenerating human annulus. Spine J 2009;9:210–5.
14. Silvan U, Diez-Torre A, Arluzea J, Andrade R, Silio M, Arechaga J. Hypoxia and pluripotency in embryonic and embryonal carcinoma stem cell biology. Differentiation 2009;78:159–68.
15. Gustafsson MV, Zheng X, Pereira T, Gradin K, Jin S, Lundkvist J, et al. Hypoxia requires Notch signaling to maintain the undifferentiated cell state. Dev Cell 2005;9:617–28.
16. Engin F, Yao Z, Yang T, Zhou G, Bertin T, Jiang MM, et al. Dimorphic effects of Notch signaling in bone homeostasis. Nat Med 2008;14:299–305.
17. Hilton MJ, Tu X, Wu X, Bai S, Zhao H, Kobayashi T, et al. Notch signaling maintains bone marrow mesenchymal progenitors by suppressing osteoblast differentiation. Nat Med 2008;14:306–14.
18. Karlsson C, Jonsson M, Asp J, Brantsing C, Kageyama R, Lindahl A. Notch and HES5 are regulated during human cartilage differentiation. Cell Tissue Res 2007;327:539–51.
19. Bao ZZ, Cepko CL. The expression and function of Notch pathway genes in the developing rat eye. J Neurosci 1997;17:1425–34.
20. Hilibrand AS, Carlson GD, Palumbo MA, Jones PK, Bohlman HH. Radiculopathy and myelopathy at segments adjacent to the site of a previous anterior cervical arthrodesis. J Bone Joint Surg Am 1999;81:519–28.
21. Diez H, Fischer A, Winkler A, Hu CJ, Hatzopoulos AK, Breier G, et al. Hypoxia-mediated activation of Dll4-Notch-Hey2 signaling in endothelial progenitor cells and adoption of arterial cell fate. Exp Cell Res 2007;313:1–9.
22. Kobayashi T, Mizuno H, Imayoshi I, Furusawa C, Shirahige K, Kageyama R. The cyclic gene Hes1 contributes to diverse differentiation responses of embryonic stem cells. Genes Dev 2009;23:1870–5.
23. Grogan SP, Olee T, Hiraoka K, Lotz MK. Repression of chondrogenesis through binding of Notch signaling proteins HES-1 and HEY-1 to N-box domains in the COL2A1 enhancer site. Arthritis Rheum 2008;58:2754–63.
24. Williams R, Nelson L, Dowthwaite GP, Evans DJ, Archer CW. Notch receptor and Notch ligand expression in developing avian cartilage. J Anat 2009;215:159–69.
25. Chen J, Imanaka N, Chen J, Griffin JD. Hypoxia potentiates

Notch signaling in breast cancer leading to decreased E-cadherin expression and increased cell migration and invasion. Br J Cancer 2010;102:351–60.
26. Akimoto M, Kameda Y, Arai Y, Miura M, Nishimaki T, Takeda A, et al. Hes1 is required for the development of craniofacial structures derived from ectomesenchymal neural crest cells. J Craniofac Surg 2010;21:1443–9.
27. Agrawal A, Guttapalli A, Narayan S, Albert TJ, Shapiro IM, Risbud MV. Normoxic stabilization of HIF-1α drives glycolytic metabolism and regulates aggrecan gene expression in nucleus pulposus cells of the rat intervertebral disk. Am J Physiol Cell Physiol 2007;293:C621–31.
28. Karlsson C, Brantsing C, Egell S, Lindahl A. Notch1, Jagged1, and HES5 are abundantly expressed in osteoarthritis. Cells Tissues Organs 2008;188:287–98.
29. Johnson WE, Eisenstein SM, Roberts S. Cell cluster formation in degenerate lumbar intervertebral discs is associated with increased disc cell proliferation. Connect Tissue Res 2001;42:197–207.
30. Sharp CA, Roberts S, Evans H, Brown SJ. Disc cell clusters in pathological human intervertebral discs are associated with increased stress protein immunostaining. Eur Spine J 2009;18:1587–94.
31. Lotz MK, Otsuki S, Grogan SP, Sah R, Terkeltaub R, D'Lima D. Cartilage cell clusters [review]. Arthritis Rheum 2010;62:2206–18.
32. Tran CM, Markova D, Smith HE, Susarla B, Ponnappan RK, Anderson DG, et al. Regulation of CCN2/connective tissue growth factor expression in the nucleus pulposus of the intervertebral disc: role of Smad and activator protein 1 signaling. Arthritis Rheum 2010;62:1983–92.
33. Hiyama A, Sakai D, Risbud MV, Tanaka M, Arai F, Abe K, et al. Enhancement of intervertebral disc cell senescence by Wnt/β-catenin signaling–induced matrix metalloproteinase expression. Arthritis Rheum 2010;62:3036–47.
34. Fu Y, Chang A, Chang L, Niessen K, Eapen S, Setiadi A, et al. Differential regulation of transforming growth factor β signaling pathways by Notch in human endothelial cells. J Biol Chem 2009;284:19452–62.
35. Corada M, Nyqvist D, Orsenigo F, Caprini A, Giampietro C, Taketo MM, et al. The Wnt/β-catenin pathway modulates vascular remodeling and specification by upregulating Dll4/Notch signaling. Dev Cell 2010;18:938–49.
36. McGill MA, McGlade CJ. Mammalian numb proteins promote Notch1 receptor ubiquitination and degradation of the Notch1 intracellular domain. J Biol Chem 2003;278:23196–203.

DOI 10.1002/art.30289

Clinical Image: Development of miliary tuberculosis following one intraarticular injection of etanercept

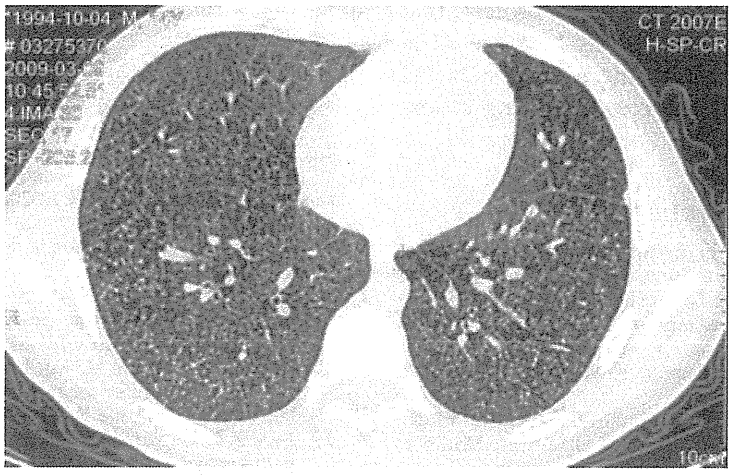

The patient, a 14-year-old boy with juvenile spondylarthritis, presented to our clinic with a 10-month history of active arthritis in his right knee joint as well as swelling of his heel. The arthritis was refractory to treatment with a combination of nonsteroidal antiinflammatory drugs, sulfasalazine, and a corticosteroid. After we confirmed that the results of a purified protein derivative (PPD) skin test and serum antitubercle bacilli antibodies (using TB-CHECK-1) were negative, a single 25-mg dose of etanercept was injected into his right knee, which resulted in rapid and dramatic improvement of the knee arthritis. Four weeks later, he developed fever (maximum temperature 39°C) and malaise. High-resolution computed tomography (HRCT) of the chest showed innumerable tiny, well-defined, miliary nodules throughout the lungs, pleural surfaces, and bronchovascular structures, which was suggestive of acute miliary pulmonary tuberculosis. Although sputum culture results were negative for *Mycobacterium tuberculosis*, the results of repeat PPD skin test and tests for tuberculosis antibodies were all positive. The patient was treated with a combination of rifampin, isoniazid, and pyrazinamide. The fever resolved after 2 weeks, the miliary nodules had nearly disappeared on repeat HRCT of the chest 3 months later, and the patient completed 1 year of antituberculosis therapy without incident.

Sheng Guang Li, MD
Chinese People's Liberation Army General Hospital
Beijing, China

Journal of Cellular Physiology

The Relationship Between the Wnt/β-Catenin and TGF-β/BMP Signals in the Intervertebral Disc Cell

AKIHIKO HIYAMA,[1,2*] DAISUKE SAKAI,[1,2] MASAHIRO TANAKA,[1] FUMIYUKI ARAI,[1] DAISUKE NAKAJIMA,[3] KOICHIRO ABE,[3] AND JOJI MOCHIDA[1,2]

[1]*Department of Orthopaedic Surgery, Surgical Science, Tokai University School of Medicine, Isehara, Kanagawa, Japan*

[2]*Research Center for Regenerative Medicine, Tokai University School of Medicine, Isehara, Kanagawa, Japan*

[3]*Department of Molecular Life Science, Division of Basic Medical Science and Molecular Medicine, Tokai University School of Medicine, Isehara, Kanagawa, Japan*

Degeneration of the lumbar intervertebral disc (IVD) is a cause of low back pain. In osteoarthritis patients, an increase in β-catenin accumulation has been reported. However, the molecular mechanisms involved in IVD remain unclear. In the present study, we examined the relationship of Wnt/β-catenin and transforming growth factor-β (TGF-β)/bone morphogenetic protein (BMP) signals in the IVDs. We found that treatment of nucleus pulposus (NP) cells with the Wnt/β-catenin activator lithium chloride (LiCl) results in the increased expression of β-catenin mRNA and protein, and cell proliferation is decreased due to the activation of the Wnt/β-catenin signals through the suppression of c-myc and cyclin-D1. In addition, T-cell-specific transcription factor (TCF) promoter activity was found to increase the following stimulation with LiCl alone, and was further increased when BMP2 was added, in comparison to the control group. We further observed the effects of treatment with PD98059, a specific inhibitor of the mitogen-activated protein kinase pathway, on TCF promoter activity in NP cells. These effects were largely attenuated by PD98059. Moreover, when transfected IVDs were co-transfected with R-Smad expression plasmids, there was a significant decrease in TCF reporter activity. We thereafter evaluated the effects of increased Wnt/β-catenin activity on the transcriptional activity of the Smad binding element (SBE). As a result, LiCl suppressed the activity of SBE reporter activity. The present study demonstrates for the first time that there are opposing effects between the Wnt/β-catenin and TGF-β/BMP signals in IVDs, which is consistent with the Wnt/β-catenin signals contributing to the pathogenesis of IVD degeneration.
J. Cell. Physiol. 226: 1139–1148, 2011.

It has been some time since the concept of discogenic low back pain was reported. Intervertebral disc (IVD) degeneration is a common cause of pain in these patients, and although the efficacy of surgical treatment is confirmed, new post-operative functional disorders have also been reported. In recent years, a regenerative medicine approach has attracted much attention (Thompson et al., 1991; Sakai et al., 2003; Masuda et al., 2004; Hiyama et al., 2008a, 2008b). However, in order to achieve consistent therapeutic effects, it is necessary to elucidate the molecular mechanism underlying the expression of IVD degeneration. The IVD acts as a shock absorber, has a jelly-like consistency in its center, or nucleus pulposus (NP) due to altered proteoglycan (PG) metabolism, and distributes pressure away from the spine and maintains the trunk. IVD cells exhibited degenerative change with advancing age. The most significant biochemical change to occur in disc degeneration is the loss of PG. Therefore, in elucidating IVD degeneration, the metabolism of IVD cells, or net change in PG content, is important. We previously reported the outcome of an analysis of the Smad proteins, in which the transforming growth factor-β (TGF-β) family was found to dominantly induce PG synthesis in IVD cells (Hiyama et al., 2008a, 2008b). Although it has been established that Smads function as a molecular switch to activate the transcription of various target genes, it is not yet clear how they become involved in IVD degeneration via dysregulated signaling. In addition, during IVD embryogenesis, the cells of the notochord play a critical role in initiating tissue formation, and may be directly responsible for development of the NP. In some species, including humans, these notochordal cells are eventually lost, usually through apoptosis or terminal differentiation, and are replaced by chondrocyte-like cells (Erwin and Inman, 2006). The free cytoplasmic β-catenin pool thereafter moves to the nucleus and activates the transcription of the T-cell-specific transcription factor (TCF)/lymphoid enhancer factor (LEF) family, which mediates the transcription of several genes encoding such proteins as c-myc and cyclin D1. The β-catenin molecule forms a complex with TCF/LEF to form a functional transcription factor (Gordon and Nusse, 2006). These interactions suggest that β-catenin may therefore play an essential role in the control of cellular proliferation, differentiation, cell polarity, adhesion, apoptosis, and tumorigenesis by regulating both cell–cell interactions and gene transcription (Nelson and Nusse, 2004; Clevers, 2006). Interestingly, (TGF-β/bone morphogenetic protein (BMP)) signals inhibits glycogen synthase kinase-3β (GSK3β) and

Additional Supporting Information may be found in the online version of this article.

Contract grant sponsor: Japan Orthopaedics and Traumatology Foundation 0120.
Contract grant sponsor: Ministry of Education, Culture, Sports, Science, and Technology of Japan.
Contract grant sponsor: Tokai University School of Medicine Research.

*Correspondence to: Akihiko Hiyama, Department of Orthopaedic Surgery, Surgical Science, Tokai University School of Medicine, Bohseidai, Isehara, Kanagawa, 259-1193, Japan. E-mail: a.hiyama@tokai-u.jp

Received 7 April 2010; Accepted 8 September 2010

Published online in Wiley Online Library (wileyonlinelibrary.com), 13 October 2010.
DOI: 10.1002/jcp.22438

activates the Wnt/β-catenin signals in various cell types (Cheon et al., 2004). The analyses of Wnt signals using mouse models have been indispensable in elucidating the formation of various organs, and many of these studies have demonstrated the importance of the β-catenin pathway (Wells et al., 2007; Harada et al., 1999). However, there have been no reports on the role of Wnt/β-catenin signals in IVD cells or on the impact of Wnt/β-catenin signals on the metabolism of IVD cells, and as a result the degenerative process remains poorly characterized.

Therefore, it is expected that the clarification of the mechanisms controlling Wnt/β-catenin signals (inhibition and activation) as well as the mechanism of Wnt/β-catenin transcriptional activation will clarify disc differentiation and the subsequent degenerative IVD process. We herein focused on Wnt/β-catenin signals, and studied the expression of these signals and the mechanisms controlling TGF-β/BMP signals, which are important for PG synthesis in IVD cells.

Materials and Methods

Plasmids and reagents

To determine the β-catenin-TCF/LEF transcriptional activity, NP cells and annlus fibrosus (AF) cells were transiently transfected with the Tcf/Lef reporter gene Topflash (optimal Tcf-binding site) or Fopflash (mutated Tcf-binding site) (Upstate Biotechnology Inc., Lake Placid, NY). The aggrecan reporter plasmid (Agg-luc) was provided by Dr. Michael C. Naski (The University of Texas Health Science Center at San Antonio). The aggrecan promoter carries 1.2 kb of the proximal mouse promoter (Reinhold et al., 2006). The Smad binding element (SBE)4-luc, SBE2-luc, and MBE6-luc plasmids, which have four copies of the Smad binding site upstream of the luciferase gene, two copies of the Smad binding site, and two copies of the mutant Smad binding site, respectively, were purchased from Addgene (Cambridge, MA) (SBE4-luc:16495, SBE2-luc:16500, and MBE6-luc:16497).The c-myc reporter plasmid (16601) was also purchased from Addgene. The R-Smad expression plasmids (Smad1, Smad2, Smad3, Smad5, and Smad8) and the empty backbone plasmid were provided by Dr. Miyazono at the University of Tokyo at Tokyo in Japan. As an internal transfection control, we used the empty vector pGL4.74 (Promega, Madison, WI) containing the *Renilla reniformis* luciferase genes. Lithium chloride (LiCl) has been shown to promote Wnt/β-catenin signals through the β-catenin pathway. In addition, Dickkopf-1 (DKK1) (R&D Systems, Minneapolis, MN) is a secreted protein that acts as a soluble inhibitor of the Wnt signaling pathway. In some experiments, to inhibit MEK activation, the MEK inhibitor PD98059 (Calbiochem, San Diego, CA) dissolved in dimethyl sulfoxide (DMSO) was added to the cell cultures.

Preparation of Wnt3A, Wnt5a-containing conditioned medium

The L-Wnt3A cell line stably expressing Wnt-3A, Wnt-5a and the control WT L-cell line were purchased from the American Type Culture Collection (Manassas, VA, USA). Medium conditioned by L-Wnt3A, L-Wnt5A or WT L-cells over a 72 h period (hereafter termed Wnt3A-containing conditioned medium (Wnt3A-CM), Wnt5A-containing conditioned medium (Wnt5A-CM) or WT-CM, respectively) were collected, processed, and used according to the manufacturer's protocol.

Isolation of intervertebral disc cells

NP and AF cells were isolated from a total of 32 female Sprague-Dawley (SD) rats (6–9 months of age) using a previously reported method (Hiyama et al., 2008a, 2008b). The gel-like NP was separated from the AF by using a dissecting microscope. The isolated cells were maintained in Dulbecco's modified Eagle's medium (DMEM) and 10% fetal bovine serum (FBS) supplemented with antibiotics in a humidified atmosphere containing 5% CO_2 at 37°C. When confluent, NP and AF cells were harvested and subcultured in 10-cm dishes. We used the low-passage (<3) cells cultured in a monolayer.

Immunofluorescence microscopy

NP cells were plated in flat-bottom 96-well plates (5,000 cells/well) and were treated with LiCl (20 mM) or BMP2 (100 ng/ml) for 24 h. After incubation, the cells were fixed with 4% paraformaldehyde, permeabilized with 0.2% Triton X-100 in phosphate buffered saline (PBS) for 10 min, blocked with PBS containing 5% FBS, and incubated with antibodies against β-catenin (1:200; catalog no. 9562; Cell Signaling, Inc, Danvers, MA), GSK3β (1:200; catalog no. 9315; Cell Signaling) or Wnt3a (1:200; catalog no. 2721; Cell Signaling) at 4°C for 18 h. After washing, the cells were incubated with anti-rabbit AlexaFluor488 secondary antibody (Invitrogen, Carlsbad, CA) at a dilution of 1:50 and 10 μm DAPI for 1 h at room temperature. The cells were imaged by laser-scanning confocal microscopy. For quantification purposes, a minimum of 100 cells, spanning five different microscopy fields, were scored for staining.

Immunohistological studies

Freshly isolated 3-week-old rat and embryonic mouse (E9.5 and E15.0) spinal tissue specimens were immediately fixed in 4% paraformaldehyde in PBS and were embedded in paraffin. Transverse and coronal sections were deparaffinized in xylenes, rehydrated through a graded ethanol series, and stained with hematoxylin and eosin. For localizing Wnt3a, sections were incubated with an anti-Wnt3a antibody (Cell Signaling) in 2% bovine serum albumin in PBS at a dilution of 1:200 at 4°C overnight. After thoroughly washing the sections, the bound primary antibody was incubated with a biotinylated universal secondary antibody, at a dilution of 1:20 (Vector Laboratories, Burlingame, CA) for 10 min at room temperature. Sections were incubated with a streptavidin/peroxidase complex for 5 min and washed with PBS, and the staining was developed using the 3′-3-diaminobenzidine substrate (Vector Stain Universal Quick Kit; Vector Laboratories).

MTT assay

The effects on cellular proliferation were measured using a modified 3-(4,5-dimethylthiazol-2-yl)-2,5-diphenyltetrazolium bromide (MTT) assay, based on the ability of live cells to utilize thiazolyl blue and convert it into the water-insoluble dark blue formazan stain. Exponentially growing NP cells were seeded into a 24-well plate at 1.5×10^4 cells/well. After LiCl stimulation (20 mM for 24–48 h), cells were treated with MTT (5 g/L, Sigma^{Q6}) for 2 h at 37°C, DMSO (Me_2SO) was added into each well, and the reaction was incubated for 30 min. Subsequently, the cells were transferred to a 96-well plate. A 96-well microtitre plate reader (GE health care, Buckinghamshire, UK) was used to quantify the A_{590}. The number of control cells that is viable cells not exposed to any treatment, was defined as 100%.

Real-time reverse transcription-polymerase chain reaction (RT-PCR) analysis

IVD cells were cultured in 6-cm dishes (5×10^5 cells/dish) 1 day before treatment with LiCl (20 mM) for 24 h. Following treatment, cells were lysed, and the total RNA was isolated using the Trizol reagent (Invitrogen). As mentioned above, cDNA was synthesized by the reverse transcription of mRNA. The real-time PCR analyses were performed in duplicate using 96-well plates with the Fast SYBR green master mix (Life Technologies, CA). Glyceraldehyde-3-phosphate dehydrogenase (GAPDH) was used as an endogenous control. Two microliters of cDNA per sample were used as a template for real-time PCR; 1 μl forward primer and 1 μl reverse primer were added to 20 μl SYBR green master mix. The reactions were synthesized in a 20-μl reaction volume with the following conditions: Initial step at 50°C for 2 min, followed by 95°C for 10 min; 40 cycles of (denaturation, 95°C for 3 s, and hybridization/elongation, at 60°C for 30 s). All primers (β-catenin, GSK3β,

cyclin-D1, c-myc, and GAPDH) were designed based on the coding sequences from Genbank (AF121265.1, NM_032080.1, NM_080782.3, NM_012603.2, and NM_017008.3, respectively), and were synthesized by Takara Bio Inc. (Tokyo, Japan). The relative quantitation of real-time RT-PCR data was performed using the delta–delta C_t method (Livak and Schmittgen, 2001). Data are reported as the average value of the range of the calculated fold difference, which incorporates the standard deviation of the delta–delta C_t value in the fold difference calculation as delta–delta C_t + SD and delta–delta C_t − SD. The statistical analyses were calculated using the SPSS software program (SPSS 14.0, Chicago, IL) using a one-way ANOVA with Tukey's HSD post-hoc pairwise comparisons ($P < 0.05$).

Transfections and dual luciferase assay

NP cells were transferred to 24-well plates at a density of 6×10^4 cells/well 1 day before transfection. The next day, to investigate the effect of LiCl and BMP2 on Topflash activity, NP cells were treated with LiCl (20 mM) or BMP2 (100 ng/ml) with 900 ng of the Topflash reporter plasmid. To evaluate Tcf transcription activity through the Smad pathway, which is downstream from the TGF-β/BMP signals, we used an expression plasmid. NP and AF cells were co-transfected with 500 ng of a R-Smad (Smad1, Smad2, Smad3, Smad5, or Smad8) or the backbone vector with 400 ng of the Topflash reporter plasmid. We then evaluated the effects of an increased Wnt/β-catenin activity on the transcription activity of the SBE4 and SBE2 promoter, which lies upstream of the luciferase gene and is the specific promoter for the target gene of the Smad complex. At the same time, we also conducted an evaluation for cases involving the MBE6 reporter, which is a mutant vector. Briefly, NP and AF cells were transfected with 900 ng of the SBE4 reporter, the SBE2 reporter or the MBE6 reporter plasmid. The cultured cells were treated with or without LiCl (20 mM) for 24 h, and the luciferase reporter activity was measured. Thereafter, to evaluate the effects of ERK signaling on the transcription activity of SBE and TCF, NP cells were treated with or without 100 ng/ml BMP2 and 1, 10, or 100 mM PD98059 with 900 ng of the Topflash reporter plasmid or 900 ng of the SBE4 reporter plasmid. In addition, to evaluate the effect of Wnt3a on the transcriptional activity of SBE and aggrecan, NP and AF cells were co-transfected with 100–500 ng of Wnt3a, or the respective empty backbone vectors, with 400 ng of SBE4 reporter plasmid or the aggrecan reporter plasmid. The pGL4.74 plasmid containing the *R. reniformis* luciferase gene was used as an internal control for normalization of all transfection experiments. Lipofectamine 2000 (Invitrogen) was used as the transfection reagent. For each transfection, plasmids were premixed with the transfection reagent. Forty-eight hours after the initial transfection, the cells were harvested and a Dual-Luciferase reporter assay system (Promega) was used for the sequential measurements of the firefly and renilla luciferase activities. Transfection efficiency for rat nucleus and annulus cells was about 50–60%. The luciferase activities and calculation of the relative ratios were quantified using a Turner Designs Luminometer Model TD-20/20 (Promega) (TD-20/20; Turner Designs, CA).

Statistical analysis

All measurements were performed in triplicate and were repeated with two independent cultures. Data are presented as the mean ± SD. To test for significance, data were analyzed using an unpaired Student's *t*-test; the obtained *P*-values are indicated in the text and figures ($^*P < 0.05$). $P < 0.05$ was considered to be statistically significant.

Results

To investigate the role of the Wnt/β-catenin signals in the IVD, we first determined whether rat IVD cells express β-catenin mRNA. Figure 1A shows that treatment for 6–24 h with LiCl (20 mM), which mimics Wnt/β-catenin signals activation, results in increased β-catenin mRNA levels in both NP and AF cells. In order to assess the relationship with TGF-β/BMP signals caused by the activation of Wnt/β-catenin signals, we performed a reporter assay to confirm the TCF activity. The results revealed the Topflash reporter activity to increase by 7.16-fold following stimulation with LiCl (20 mM), and was further increased by 9.5-fold when BMP2 (100 ng/ml) was added, when compared to the control group (Fig. 1B). In addition, we determined the expression levels of the β-catenin protein in rat NP cells following treatment with LiCl (20 mM) or BMP2 (100 ng/ml). As shown in Figure 1C, an immunofluorescence analysis with an anti-β-catenin antibody demonstrated that LiCl and BMP2 treatment induces the expression of total β-catenin levels and promotes the nuclear translocation of β-catenin in NP cells. LiCl and BMP2 treatment for 24 h increased the average proportion of β-catenin-positive NP cells (LiCl) compared to untreated controls (Cr) (LiCl: 84.51 ± 4.45%, BMP2: 53.34 ± 3.50%, Cr: 39.04 ± 9.82%; $P < 0.05$). To further explore the effect of LiCl suppression on GSK3β gene and protein expression in NP cells, we performed a real-time PCR and immunofluorescence analysis.
Figure 1D shows that there is a marked suppression in GSK3β mRNA levels when NP cells were treated with LiCl (20 mM), and an immunofluorescence analysis showed the cytoplasmic staining to decrease by treatment with an anti-GSK3β antibody in LiCl-treated NP cells. From these data, we demonstrated that the inhibition of GSK3β by LiCl induced the nuclear translocation of β-catenin in NP cells.

Furthermore, when NP and AF cells were co-transfected with R-Smad expression plasmids, a significant decrease was observed in the Topflash reporter activity both in NP cells (Fig. 2A) and in AF cells (Fig. 2B). We thereafter evaluated the effects of increased Wnt/β-catenin activity on the transcriptional activity of the SBE4 reporter and the SBE2 reporter, in which the luciferase genes lie downstream of the SBE, which is the specific promoter for the target genes of the Smad complex. At the same time, we also conducted an evaluation for cases involving the MBE6 reporter, which is a mutant vector. As a result, treatment with LiCl inhibited SBE4 and SBE2 reporter activity, whereas the MBE6 reporter failed to suppress activity both in NP cells (Fig. 2C) and in AF cells (Fig. 2D). The ERK signaling cascade transmits signals from a variety of extracellular stimuli to multiple cellular processes, including cell proliferation, differentiation, and development. Recently, the existence of crosstalk between Wnt and ERK pathways was reported. Therefore, we further examined the effect of mitogen-activated protein kinase signaling on TCF reporter activity in NP cells. NP cells were transfected with the Topflash or SBE4 reporter plasmid and treated with BMP2 or LiCl and PD98059 for 24 h. PD98059 prevented the BMP2 or LiCl-induced increase in Topflash and SBE4 reporter activity (Fig. 3A–C). In addition, to investigate the further effect of Wnt/β-catenin signals, we analyzed ERK1 and ERK2 mRNA expression by real-time PCR. Figure 3D shows that treatment with LiCl (20 mM) for 24 h resulted in decreased ERK1 and ERK2 mRNA levels in NP cells. Conversely, ERK1 and ERK2 mRNA levels were not affected by LiCl treatment in AF cells (Fig. 3E).

In addition, we determined whether the treatment of NP cells with LiCl (20 mM) resulted in a decreased cell proliferation. An MTT assay was performed to assess the rates of Wnt/β-catenin-induced NP cell proliferation.
Figure 4A shows that cell proliferation decreased due to the activation of the Wnt/β-catenin signals compared to untreated controls (24 h; 70.39 ± 3.19%, control; 100 ± 7.25%, 48 h; 92.27 ± 7.00%, control; 164.67 ± 3.5%). Furthermore, we determined the expression levels of c-myc and cyclin-D1

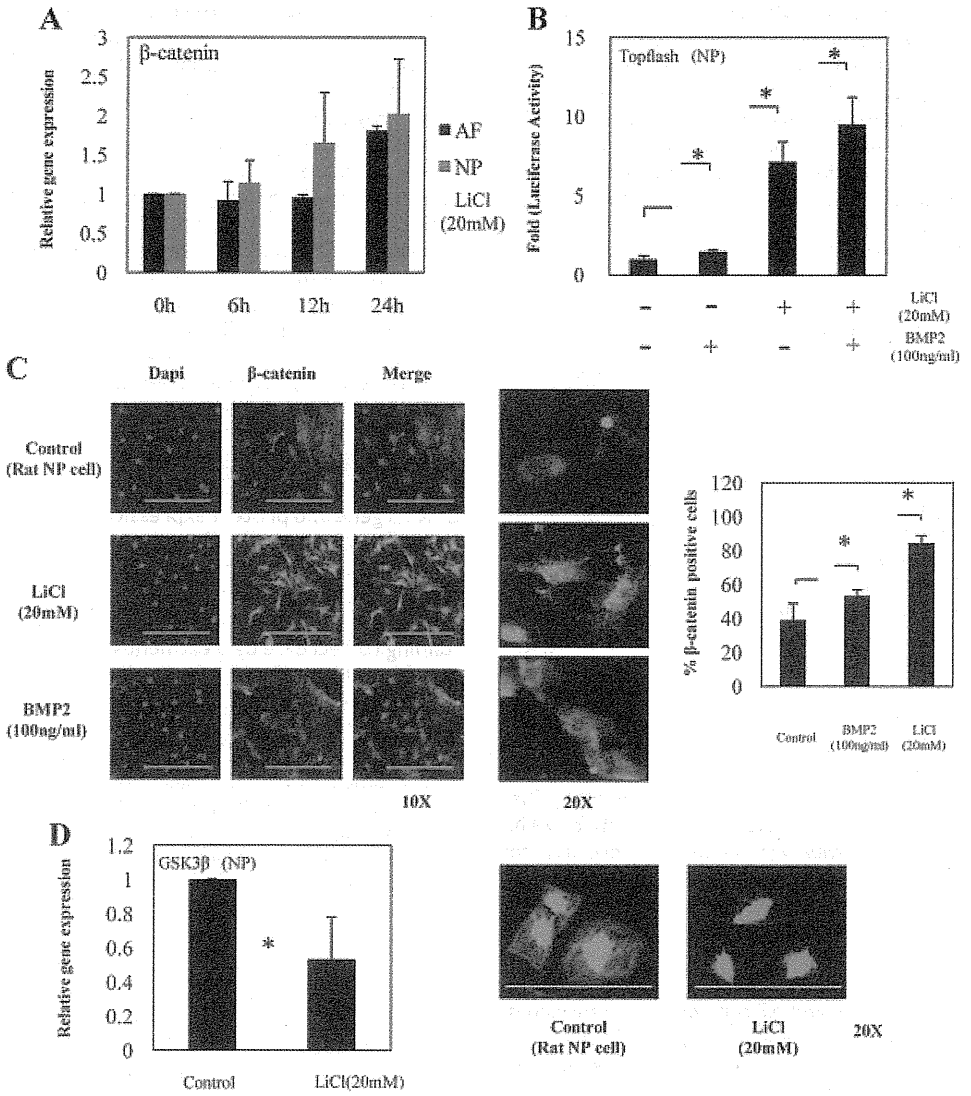

Fig. 1. LiCl and BMP2 activate β-catenin expression in IVD cells. A: Real-time RT-PCR of β-catenin mRNA levels in the presence or absence of 20 mM LiCl for 6–24 h, both in NP cells and AF cells. B: NP cells were co-transfected with the Topflash reporter plasmid and the pGL4.74 vector, and were treated with LiCl (20 mM) or BMP2 (100 ng/ml). The luciferase activity was measured 24 h after transfection. C: Confocal imaging of β-catenin nuclear translocation in NP cells after treatment with LiCl (20 mM) or BMP2 (100 ng/ml) for 24 h. Left: Cells were stained with DAPI to identify healthy nuclei. Middle: Cells stained with an antibody to β-catenin. Right: Cells stained with β-catenin and DAPI. Scale bar: 200 μm (original magnification 10× or 20×). D: Real-time reverse transcription-polymerase chain reaction of GSK3β mRNA levels in the presence or absence of LiCl (20 mM) for 24 h in NP cells. NP cells were stained for immunofluorescence with the anti-GSK3β and fluorescent-labeled secondary antibodies (right). Scale bar: 200 μm (original magnification 20×). The values represent the mean ± SD of three independent experiments (*$P < 0.05$).

mRNA, which regulate cell proliferation following treatment with LiCl (20 mM). Figure 4B shows that treatment with LiCl for 24 h results in decreased c-myc and cyclin-D1 mRNA levels in NP cells. This result was similar to the c-myc reporter activity observed following LiCl treatment (Fig. 4C). We next examined the morphological changes in NP cells after exposure to LiCl (20 mM) or DKK1 (100 ng/ml) (Fig. 4D). Figure 4D shows that treatment with LiCl decreased the number of NP cells, whereas treatment with DKK1 did not decrease the number of NP cells. In addition, there was no marked influence on the cellular morphology.

We further investigated the role of the Wnt ligand in the IVD, and first determined whether rat IVDs express Wnt3a. Wnt3a is a secreted ligand and activates members of the Frizzled family of receptors. Wnt3a is one of the closely related Wnt family members and has multiple roles in development and cell fate. Recently, some groups have reported that Wnt3a induces the expression of chondrocyte marker genes, and is a key regulator of the chondrocyte life cycle during embryonic development. Figure 5A shows the expression of Wnt3a in the neonatal rat (3 weeks of age) and embryonic mouse (day E9.5 and E15.0). The immunohistological analyses revealed that Wnt3a is expressed in notochordal cells and NP cells. Much of the staining was nuclear. However, some staining was observed in the cytosol of the NP cells. In addition, we determined the expression levels of Wnt3a protein in rat NP cells following treatment with LiCl (20 mM) or BMP2 (100 ng/ml). As shown in Figure 5B, the immunofluorescence analyses with an anti-Wnt3a antibody

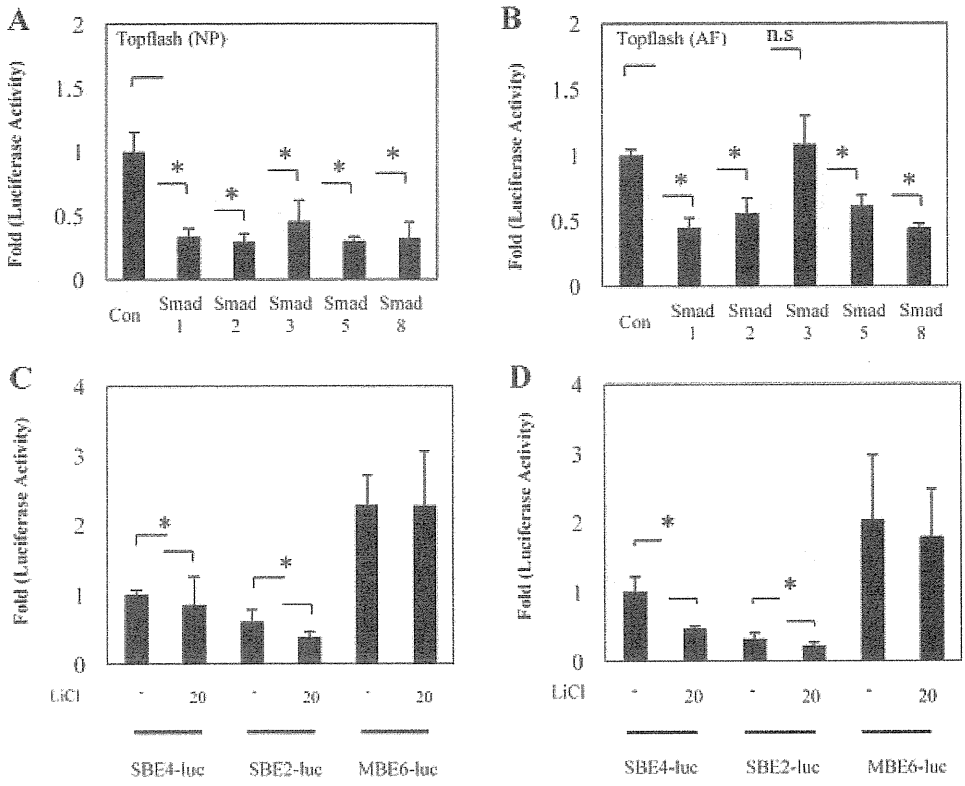

Fig. 2. The TGF-β/BMP and Wnt/β-catenin signals produce opposite effects. A, B: Subconfluent rat NP (A) and AF (B) cells were co-transfected with the Topflash reporter plasmid (400 ng) with either R-Smad expression plasmids (500 ng) or the respective empty backbone vectors (500 ng). The cells were cultured for 48 h after transfection, and reporter activity was measured. C, D: The SBE4 reporter (900 ng), the SBE2 reporter (900 ng), or the MBE6 reporter (900 ng) were transfected into rat NP (C) and AF (D) cells along with the pGL4.74 vector (100 ng). The cultured cells were treated with LiCl (20 mM) for 24 h and luciferase reporter activity was measured thereafter. The values represent the mean ± SD of three independent experiments (*$P < 0.05$).

demonstrated that LiCl or BMP2 treatment induced total Wnt3a protein expression and promoted the nuclear translocation of Wnt3a in NP cells. To further evaluate the activation of Wnt3a, we measured the activity of the Topflash reporter in NP and AF cells. These cells were transfected with plasmids encoding TCF and were treated with Wnt3A-CM, a Wnt protein that signals through β-catenin; companion cultures received a control vehicle, medium (WT-CM), or DKK1. Figure 5C shows that Topflash reporter activity was induced 50-fold in Wnt3A-CM-treated cultures within 24 h in NP cells. In contrast, Topflash reporter activity was activated by 10-fold in Wnt3A-CM-treated cultures within 24 h in AF cells. DKK1 addition suppressed Topflash reporter activity. Similar levels of reporter activity were elicited by treatment with the Wnt3a expression plasmid (data not shown).

In order to determine whether the Wnt3a protein directly interacts with BMP-2 and TGF-β signaling, the SBE4 reporter plasmid was co-transfected with the WT-Wnt3a expression plasmid into NP and AF cells. Figure 5D shows that SBE4 reporter activity is unresponsive to Wnt3a treatment in a dose-dependent manner in both NP and AF cells. To understand the Wnt/β-catenin signals in IVD cells, we also examined the Wnt5a protein, which stimulates non-canonical Wnt signaling. Both NP and AF cells were transiently transfected with either the Topflash reporter or the Fopflash reporter along with the pGL4.74 vectors. The cultured cells were treated with either Wnt3a- or Wnt5a-CM for 24 h, and luciferase reporter activity was measured. Figure 6A shows that Topflash reporter activity is activated by Wnt3a-CM treatment both in NP cells and in AF cells, whereas Topflash reporter activity is not affected by Wnt5a-CM treatment.

In aging IVDs, there is a well-recognized loss of cells, PG, and type II collagen. While the loss of PG is the primary chemical change in IVD degeneration present in lower back pain patients, little is known concerning the events that control this loss. Therefore, to further investigate the possible mechanisms of Wnt3a or Wnt5a protein in NP cells, we examined the effect of Wnt3a or Wnt5a protein treatment on aggrecan promoter activity in NP cells. We measured the basal activity of the aggrecan reporter in IVD cells. Figure 6B shows that NP cells displayed a significantly higher (1.8-fold) basal level of aggrecan reporter activity than AF cells. We then determined if Wnt3a or Wnt5a mediated its effects on aggrecan through the Wnt/β-catenin signals. Figure 6C shows that when NP cells were co-transfected with the aggrecan reporter plasmid and either WT-Wnt3a or WT-Wnt5a or the respective empty backbone vectors, the aggrecan reporter activity was not affected in a dose-dependent manner by either WT-Wnt3a or by the WT-Wnt5a expression plasmids.

Discussion

The purpose of the present study was to clarify the mechanisms controlling the inhibition and activation of the Wnt/β-catenin signals and the mechanism of its transcriptional activation. Therefore, we conducted an analysis of the crosstalk between

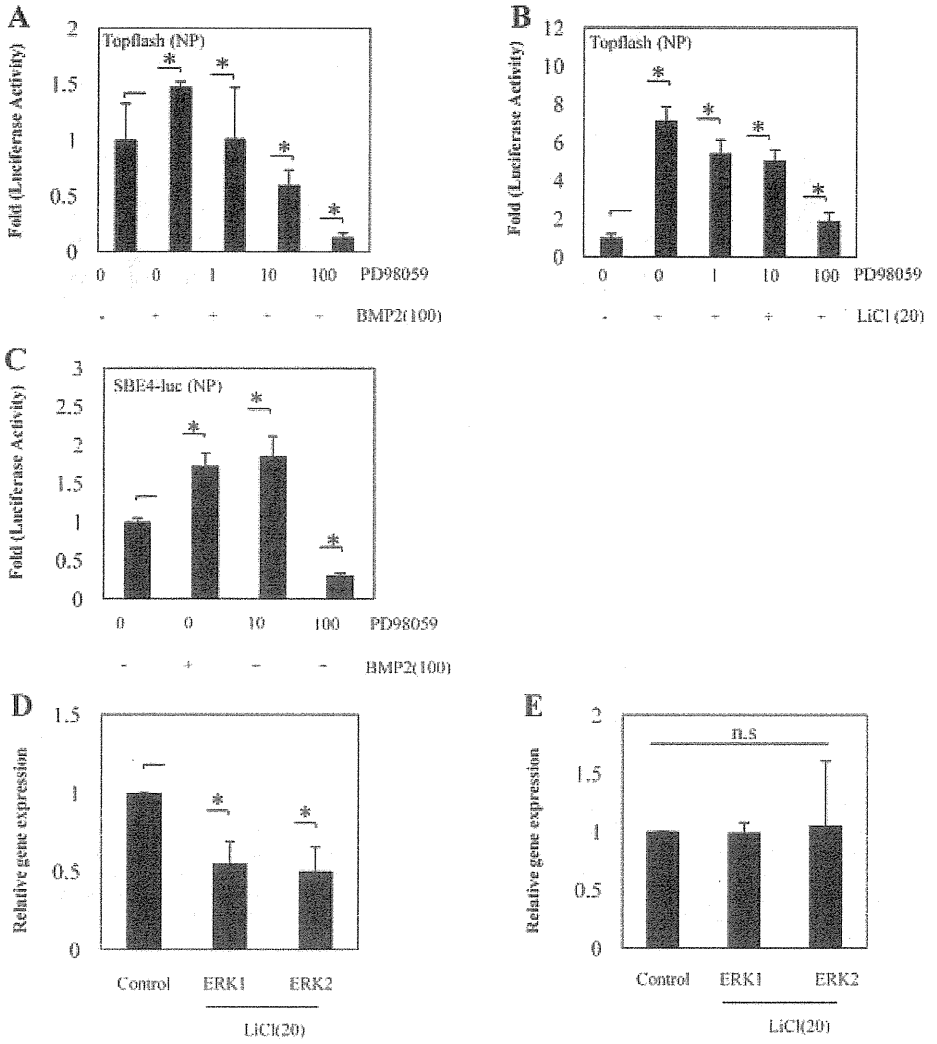

Fig. 3. Extracellular signal regulated-kinase (ERK) pathways regulate the Wnt/β-catenin signals. A, B: The Topflash reporter plasmid was transfected into rat NP cells along with the pGL4.74 vector, and was stimulated with BMP-2 (A) or LiCl (B) in the presence or absence of PD98059. Luciferase activity was measured 24 h after transfection. C: The SBE4 reporter plasmid was transfected into rat NP cells along with the PGL4.74 vector, and was stimulated with BMP-2 in the presence or absence of PD98059. The luciferase activity was measured 24 h after transfection. D, E: Total RNA from stimulated rat NP (D) and AF (E) cells was extracted and reverse transcribed into cDNA followed by real-time PCR, quantified, and normalized to untreated cells, which was arbitrarily set at 1.0. Values were normalized to the levels of GAPDH. The relative expression levels of ERK1, ERK2, and GAPDH were determined.

TGF-β/BMP signals, which was found to be important for PG synthesis in IVD cells.

However, there was a limitation with respect to the analyses and data that may affect the accuracy of these results. The limitation of the present study is the fact that we used LiCl to activate Wnt/β-catenin signaling. Selectivity is a key issue when GSK-3 inhibitors are used as pharmacological tools to demonstrate the involvement of GSK-3 in a cellular process. The selectivity of most of the available GSK-3 inhibitors is poorly known. At least 30 small molecule GSK-3 inhibitors have been developed (Alonso and Martinez, 2004; Meijer et al., 2004). Among those, LiCl has been widely used for research purposes. Clinically, lithium salts are prescribed for treatment of bipolar disorders, depression, and mania. GSK3β was firstly identified as a target of LiCl in 1996 (Klein and Melton, 1996). Several groups have used LiCl, an inhibitor of GSK3β (Berridge et al., 1989; Stambolic et al., 1996; Spencer et al., 2006), to examine these relationships. Inhibition of GSK3β leads to the accumulation of β-catenin and the activation of Wnt/β-catenin-dependent signals. It is important to note that GSK3β has other functions and that LiCl is therefore not specific for just activating the Wnt/β-catenin signals alone (Crabtree and Olson, 2002). However, we do not know the mechanism to regulate Wnt/β-catenin by LiCl in IVD. Therefore, we used LiCl as Wnt/β-catenin activator to get the first data. Moreover, we used WT-β-catenin instead of LiCl treatment, and also evaluated the effect of WT-β-catenin on reporter activity. These data were similar to results of LiCl treatment (data not shown). It means that activity of LiCl produced activation of Wnt/β-catenin signal.

First, in order to study whether NP cells express the TCF factors necessary for β-catenin-mediated transcriptional activation, LiCl was added to measure the levels of β-catenin nuclear translocation, and the transcriptional activation of Topflash. With GSK3β inhibition, the levels of β-catenin nuclear translocation and activation of Topflash substantially

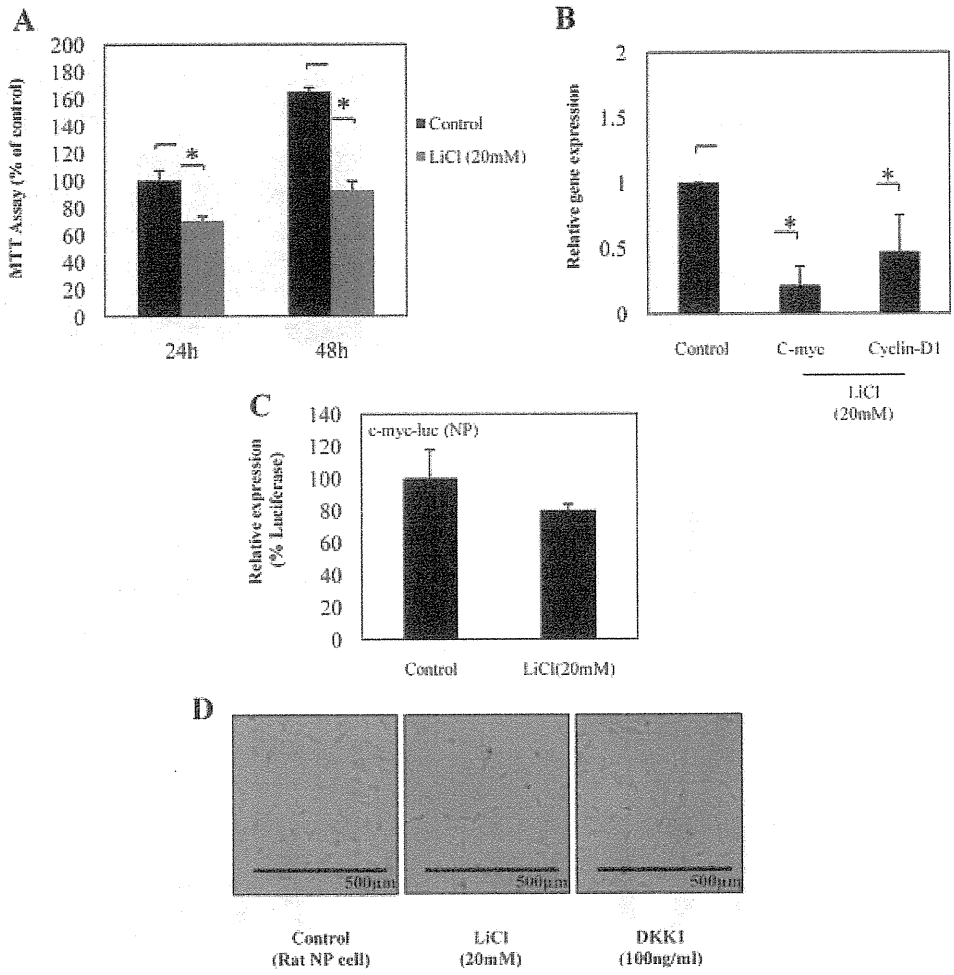

Fig. 4. The Wnt/β-catenin signals suppress IVD cell proliferation. A: The effect on cellular proliferation was also measured using the MTT assay as described in the Materials and Methods Section. *Statistically significant changes compared with the controls. B: We examined the effect of Wnt/β-catenin signaling on the expression levels of c-myc and cyclin-D1 in NP cells. The relative expression levels of c-myc, cyclin-D1, and GAPDH were determined by a real-time PCR analysis, quantified, and normalized to untreated cells, whose expression values were set to 1.0. GSK3β inhibition (activation of Wnt/β-catenin signals) caused suppression in c-myc and cyclin-D1 mRNA. C: The c-myc reporter (900 ng) was transfected into rat NP cells along with the pGL4.74 vector (100 ng). The cultured cells were treated with LiCl (20 mM) for 24 h and luciferase reporter activity was measured thereafter. D: Micrographs of NP cells harvested from 12-week-old SD rats were cultured in medium in the presence or absence of LiCl (20 mM) or DKK1 (100 ng/ml) for 24 h. Scale bar: 500 μm. The represented values indicate the mean ± SD of three independent experiments (*$P < 0.05$).

increased. In addition, when BMP2 was added with LiCl, Topflash activation increased further. This suggested that Wnt/β-catenin signals were important in IVD cells, and that TGF/BMP signal was involved in the activation of Wnt/β-catenin signals. The TGF-β superfamily binds to a type 2 receptor, a specific receptor existing on the membrane surface, and the bound type 2 receptor forms a complex with a type 1 receptor (Wrana et al., 1994; Zhang et al., 1996). Thereafter, when the type 1 receptor kinase is activated, it phosphorylates R-Smads, which are intracellular signal transduction molecules. The R-Smads include Smad2 and Smad3, which transmit TGF-β/activin signals, and Smad1, Smad5, and Smad8, which transmit BMP signals. When phosphorylated, R-Smads are able to bind to Smad4, called the Co-Smad, and the R-Smad/Co-Smad complexes formed in the cytoplasm can then enter the nucleus (Macías-Silva et al., 1996; Massagué, 1998). It is believed that once in the nucleus, the Smad complexes bind to SBEs in the promoters of target genes and, together with other transcription factors and transcription coupling factors, regulate the expression of these genes. Therefore, we focused on the Smad component of TGF/BMP signals and analyzed the R-Smad-mediated interaction of β-catenin. When R-Smad expression plasmids were transfected into IVD cells, Topflash activation markedly decreased. Furthermore, when IVD cells were treated with LiCl, the transcriptional activation of SBE was also inhibited. These results suggested that the Smad signal and the Wnt/β-catenin signals inhibit one another, and that they are involved in the maintenance of IVD homeostasis. However, it was confirmed that Topflash activation increases with the addition of BMP2, suggesting that Wnt/β-catenin signal activation is regulated by Smad-independent signals. Recently, the ERK inhibitor PD98059 was shown to prevent the inhibition of GSK3β and the nuclear accumulation of β-catenin induced by TGF-β/BMP signals (Grimes and Jope, 2001; Ding et al., 2005). Therefore, in the present study, in order to examine whether BMP-mediated activation of Wnt/β-catenin signals is induced by

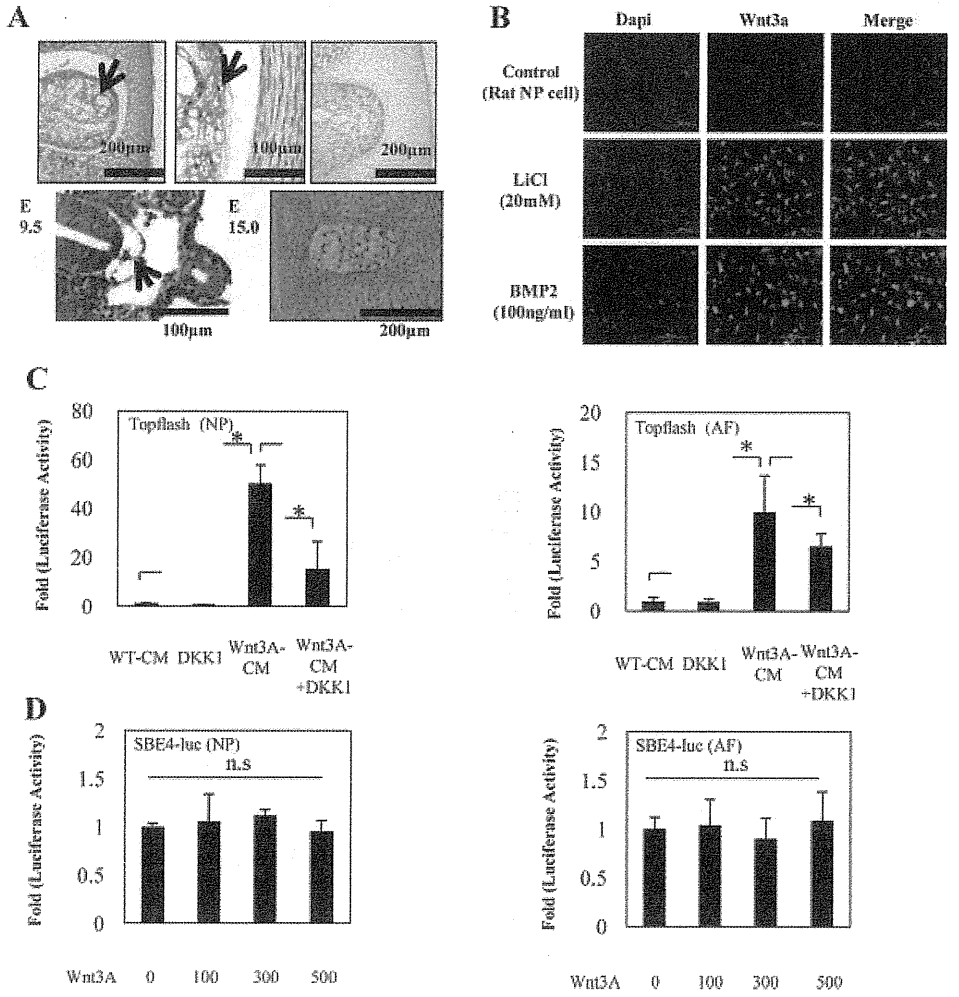

Fig. 5. Wnt3a is expressed in the IVD and activates Wnt/β-catenin signals. A: Sagittal sections of the IVD of neonatal rat (upper) and embryonic mouse (E9.5 and E15.0) (lower). Sections were treated with an anti-Wnt3a antibody and were counterstained with hematoxylin. Note that NP cells express Wnt3a protein (arrows in A). The original magnification is 10× or 20×. B: Detection of Wnt3a expression in NP cells by immunofluorescence microscopy after culturing cells with LiCl (20 mM) or BMP2 (100 ng/ml) for 24 h. Left: Cells were stained with DAPI to identify healthy nuclei. Middle: Cells stained with an antibody to Wnt3a. Right: Cells stained with Wnt3a and DAPI. Scale bar: 200 μm. C: The Topflash reporter plasmid was transfected into rat NP and AF cells along with the pGL4.74 vector, and were stimulated with DKK1 (100 ng/ml) or Wnt3A-CM for 24 h. D: Wnt3a was co-transfected with the SBE4 reporter into NP and AF cells.

ERK, PD98059 was used to inhibit ERK, therefore resulting in the concentration-dependent inhibition of the activation of Topflash and also suggesting the involvement of ERK in the activation of Wnt/β-catenin signals.

Furthermore, LiCl treatment was used to activate the Wnt/β-catenin signals, and the expression of both ERK1 and ERK2 genes was found to be markedly inhibited, thereby indicating the inhibitory involvement of the Wnt/β-catenin signals in TGF/BMP signaling. These data show that there was a time-lag between ERK1/2 or GSK3β phosphorylation and the nuclear translocation of β-catenin in response to BMP2 and LiCl. This may reflect a slow nuclear translocation of β-catenin following ERK1/2 activation/GSK3β inhibition.

Furthermore, in regard to the decrease in the number of cells, which is another important factor of IVD degeneration, it was found that the activation of Wnt/β-catenin signals led to cytostatic activity. With aging, notochord-like cells in the NP decreased in number and amyloid-like tissue replaced NP. We hypothesized that, with the activation of the Wnt/β-catenin signals, β-catenin target genes c-myc and cyclin-D1 may be involved in the initiation of cytostatic activity. It was previously suggested that Wnt signaling can promote both the c-myc and cyclin-D1 genes by the upregulation of β-catenin (He et al., 1998; Shtutman et al., 1999). Therefore, we analyzed the expression of these genes by a real-time PCR analysis and found that the expression was significantly inhibited, thereby indicating that these transcription factors regulate the growth of IVD cells. The results of the studies described herein suggest that this mechanism may be cell-specific, and LiCl may induce another pathway to suppress c-myc and cyclin-D1 gene expression.

Thereafter, stimulation by Wnt3a, the primary Wnt member of the Wnt/β-catenin signaling family, resulted in increased Topflash promoter activity and cytostatic effects, as observed with LiCl treatment, whereas a similar experiment using the Wnt antagonist Dickkopf (DKK)-1 did not induce any changes in activation. This finding suggested that the cytostatic activity in IVD cells by Wnt3a is mediated by Wnt/β-catenin signals. In

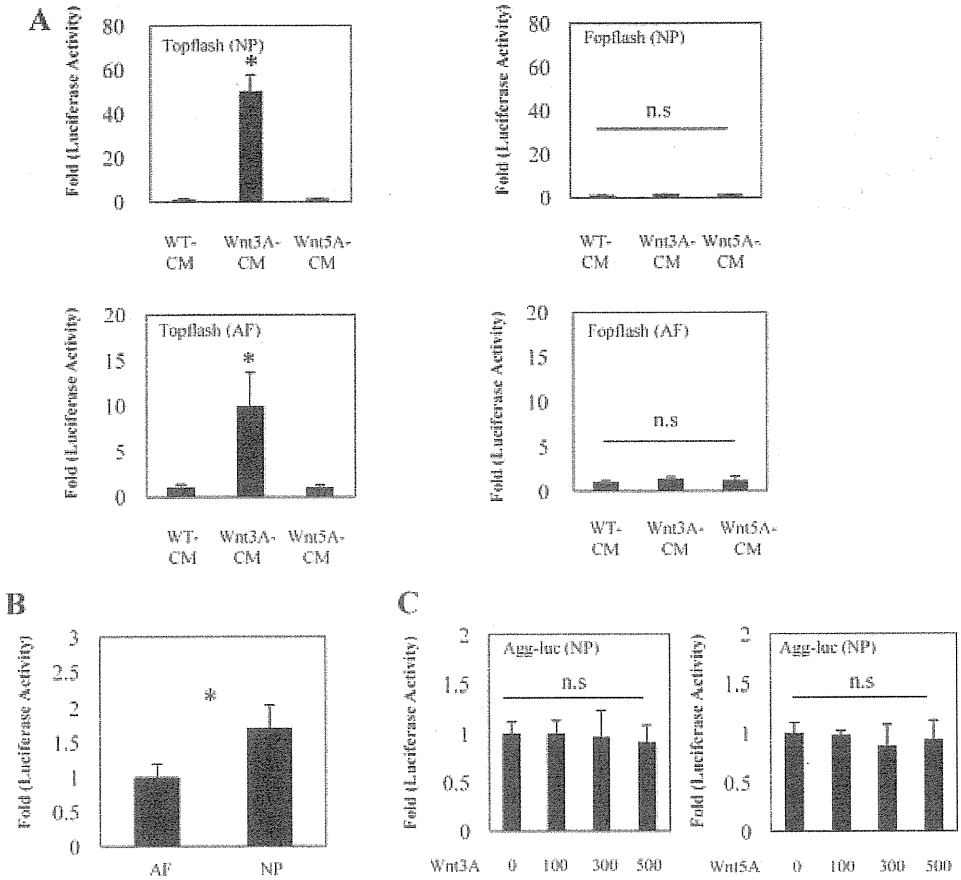

Fig. 6. Wnt3a and Wnt5a do not regulate aggrecan promoter activity. A: In order to define a functional mechanism between the Wnt3a and Wnt5a in NP cells (upper) and AF (lower) cells, cells were transfected with the Topflash (900 ng) or the Fopflash (900 ng) reporter plasmid and were treated with Wnt3A-CM or Wnt5A-CM. B: The aggrecan reporter plasmid was transfected into rat NP and AF cells along with the pGL4.74 vector, and the basal activities of the reporter were measured by a dual luciferase assay. C: NP cells were co-transfected with the aggrecan reporter plasmid with either Wnt3a, Wnt5a or empty vectors. The cells were cultured for 48 h after transfection, and the reporter activity was measured thereafter.

addition, the Topflash reporter activity for Wnt3a in NP cells was higher than that in AF cells. Their discovery suggests for the first time NP cells may have a high affinity for the Wnt3a protein than AF cells.

However, Wnt3a was not involved in PG synthesis associated with degeneration or regeneration of the IVD or in TGF/BMP signals crosstalk. Furthermore, the activation of Topflash was not observed after Wnt5a treatment, which activates a β-catenin-independent pathway, and Wnt5a was not found to be involved in the growth of cells (data not shown). Furthermore, Wnt5a was not involved in PG synthesis, as observed with Wnt3a.

In summary, based on the present findings, we concluded that the Smad signal and the Wnt/β-catenin signals inhibit each other, and that they are involved in the maintenance of IVD homeostasis. The present findings suggested that activation of Wnt/β-catenin signals by BMP2 may be regulated by Smad-independent signals. Furthermore, we have shown, for the first time, β-catenin target both genes c-myc and cyclin-D1 probably due to the stability of the NP cells in terms of cell proliferation. However, Wnt3a and Wnt5a were not involved in the PG synthesis associated with either the degeneration or regeneration of the NP cells using reporter assays. These results showed that different signal pathways might thus be involved in the regulation of the cell proliferation and PG synthesis in NP cells. However, we did not suggest whether the decrease of the cell number participated with low back pain from this study. We will think that it is necessary to investigate the relationship with low back pain and IVD degeneration at the molecular level in the future study. In addition, future studies will address the role of c-myc and cyclin-D1 and determine whether the regulation of cell growth by Wnt/β-catenin signals is specific to IVD cells.

Acknowledgments

We thank Dr. Kohei Miyazono and Dr. Michael C. Naski for kindly providing necessary reagents. We also thank Dr. Tadayuki Sato for helpful advice and excellent technical assistance. This work was supported by the Japan Orthopaedics and Traumatology Foundation (Grant 0120), a Grant-in-Aid for Scientific Research, and a Grant of The Science Frontier Program from the Ministry of Education, Culture, Sports, Science, and Technology of Japan and a grant from Tokai University School of Medicine Research.

Literature Cited

Alonso M, Martinez A. 2004. GSK-3 inhibitors: Discoveries and developments. Curr Med Chem 11:755–763.

Berridge MJ, Downes CP, Hanley MR. 1989. Neural and developmental actions of lithium: A unifying hypothesis. Cell 59:411–419.
Cheon SS, Nadesan P, Poon R, Alman BA. 2004. Growth factors regulate beta-catenin-mediated TCF-dependent transcriptional activation in fibroblasts during the proliferative phase of wound healing. Exp Cell Res 293:267–274.
Clevers H. 2006. Wnt/beta-catenin signaling in development and disease. Cell 127:469–480.
Crabtree GR, Olson EN. 2002. NFAT signaling: Choreographing the social lives of cells. Cell 109:S67–S79.
Ding Q, Xia W, Liu JC, Yang JY, Lee DF, Xia J, Bartholomeusz G, Li Y, Pan Y, Li Z, Bargou RC, Qin J, Lai CC, Tsai FJ, Tsai CH, Hung MC. 2005. Erk associates with and primes GSK-3beta for its inactivation resulting in upregulation of beta-catenin. Mol Cell 19:159–170.
Erwin WM, Inman RD. 2006. Notochord cells regulate intervertebral disc chondrocyte proteoglycan production and cell proliferation. Spine 31:1094–1099.
Gordon MD, Nusse R. 2006. Wnt signaling: Multiple pathways, multiple receptors, and multiple transcription factors. J Biol Chem 281:22429–22433.
Grimes CA, Jope RS. 2001. The multifaceted roles of glycogen synthase kinase 3 beta in cellular signaling. Prog Neurobiol 65:391–426.
Harada N, Tamai Y, Ishikawa T, Sauer B, Takaku K, Oshima M, Taketo MM. 1999. Intestinal polyposis in mice with a dominant stable mutation of the beta-catenin gene. EMBO J 18:5931–5942.
He TC, Sparks AB, Rago C, Hermeking H, Zawel L, da Costa LT, Morin PJ, Vogelstein B, Kinzler KW. 1998. Identification of c-MYC as a target of the APC pathway. Science 281:1509–1512.
Hiyama A, Mochida J, Omi H, Serigano K, Sakai D. 2008. Cross talk between Smad transcription factors and TNF-alpha in intervertebral disc degeneration. Biochem Biophys Res Commun 369:679–685.
Hiyama A, Mochida J, Iwashina T, Omi H, Watanabe T, Serigano K, Tamura F, Sakai D. 2008. Transplantation of mesenchymal stem cells in a canine disc degeneration model. J Orthop Res 26:589–600.
Klein PS, Melton DA. 1996. A molecular mechanism for the effect of lithium on development. Proc Natl Acad Sci USA 93:8455–8459.
Livak KJ, Schmittgen TD. 2001. Analysis of relative gene expression data using real-time quantitative PCR and the 2(-delta delta C(T)) method. Methods 25:402–408.
Macías-Silva M, Abdollah S, Hoodless PA, Pirone R, Attisano L, Wrana JL. 1996. MADR2 is a substrate of the TGFbeta receptor and phosphorylation is required for nuclear accumulation and signaling. Cell 87:1215–1224.
Massagué J. 1998. TGF-beta signal transduction. Annu Rev Biochem 67:753–791.
Masuda K, Oegema TR, Jr., An HS. 2004. Growth factors and treatment of intervertebral disc degeneration. Spine 29:2757–2769.
Meijer L, Flajolet M, Greengard P. 2004. Pharmacological inhibitors of glycogen synthase kinase 3. Trends Pharmacol Sci 25:471–480.
Nelson WJ, Nusse R. 2004. Convergence of Wnt, beta-catenin, and cadherin pathways. Science 303:1483–1487.
Reinhold MI, Kapadia RM, Liao Z, Naski MC. 2006. The Wnt-inducible transcription factor Twist1 inhibits chondrogenesis. J Biol Chem 281:1381–1388.
Sakai D, Mochida J, Yamamoto Y, Nomura T, Okuma M, Nishimura K, Nakai T, Ando K, Hotta T. 2003. Transplantation of mesenchymal stem cells embedded in Atelocollagen gel to the intervertebral disc: A potential therapeutic model for disc degeneration. Biomaterials 24:3531–3541.
Shtutman M, Zhurinsky J, Simcha I, Albanese C, D'Amico M, Pestell R, Ben-Zéev A. 1999. The cyclin D1 gene is a target of the beta-catenin/LEF-1 pathway. Proc Natl Acad Sci USA 96:5522–5527.
Spencer GJ, Utting JC, Etheridge SL, Arnett TR, Genever PG. 2006. Wnt signalling in osteoblasts regulates expression of the receptor activator of NFkappaB ligand and inhibits osteoclastogenesis in vitro. J Cell Sci 119:1283–1296.
Stambolic V, Ruel L, Woodgett JR. 1996. Lithium inhibits glycogen synthase kinase-3 activity and mimics wingless signalling in intact cells. Curr Biol 6:1664–1668.
Thompson JP, Oegema TR, Jr., Bradford DS. 1991. Stimulation of mature canine intervertebral disc by growth factors. Spine 16:253–260.
Wells JM, Esni F, Boivin GP, Aronow BJ, Stuart W, Combs C, Sklenka A, Leach SD, Lowy AM. 2007. Wnt/beta-catenin signaling is required for development of the exocrine pancreas. BMC Dev Biol 12:4.
Wrana JL, Attisano L, Wieser R, Ventura F, Massagué J. 1994. Mechanism of activation of the TGF-beta receptor. Nature 370:341–347.
Zhang Y, Feng X, We R, Derynck R. 1996. Receptor associated Mad homologues synergize as effectors of the TGFb response. Nature 383:168–172.

Effect of Cell Number on Mesenchymal Stem Cell Transplantation in a Canine Disc Degeneration Model

Kenji Serigano,[1,2] Daisuke Sakai,[1,2] Akihiko Hiyama,[1,2] Futoshi Tamura,[1,2] Masahiro Tanaka,[1,2] Joji Mochida[1,2]

[1]Department of Orthopaedic Surgery, Surgical Science, Tokai University School of Medicine, Shimokasuya 143, Isehara, Kanagawa 259-1193, Japan, [2]Center for Regenerative Medicine, Tokai University School of Medicine, Shimokasuya 143, Isehara, Kanagawa 259-1193, Japan

Received 8 July 2009; accepted 16 February 2010
Published online 22 April 2010 in wileyonlinelibrary.com. DOI 10.1002/jor.21147

ABSTRACT: Transplantation of mesenchymal stem cells (MSCs) inhibits the progression of disc degeneration in animal models. We know of no study to determine the optimal number of cells to transplant into the degenerated intervertebral disc (IVD). To determine the optimal donor cell number for maximum benefit, we conducted an in vivo study using a canine disc degeneration model. Autologous MSCs were transplanted into degenerative discs at 10^5, 10^6, or 10^7 cells per disc. The MSC-transplanted discs were evaluated for 12 weeks using plain radiography, magnetic resonance imaging, and gross and microscopic evaluation. Preservation of the disc height, annular structure was seen in MSC-transplantation groups compared to the operated control group with no MSC transplantation. Result of the number of remaining transplanted MSCs, the survival rate of NP cells, and apoptosis of NP cells in transplanted discs showed both structural microenvironment and abundant extracellular matrix maintained in 10^6 MSCs transplanted disc, while less viable cells were detected in 10^5 MSCs transplanted and more apoptotic cells in 10^7 MSCs transplanted discs. The results of this study demonstrate that the number of cells transplanted affects the regenerative capability of MSC transplants in experimentally induced degenerating canine discs. It is suggested that maintenance of extracellular matrix by its production from transplanted cells and/or resident cells is important for checking the progression of structural disruption that leads to disc degeneration. ©2010 Orthopaedic Research Society. Published by Wiley Periodicals, Inc. J Orthop Res 28: 1267–1275, 2010

Keywords: intervertebral disc; mesenchymal stem cells; regenerative medicine; disc degeneration; nucleus pulposus

Degenerative spinal disease not only causes lumbar pain in individuals, but also has a major socioeconomic impact from stress on the medical system and loss of productivity from occupational disease.[1,2] While intervertebral disc (IVD) degeneration has been implicated as one of the major causes of degenerative spinal disease, other factors thought to be involved including age, trauma, genetic predisposition, and lifestyle factors, such as obesity, smoking, occupation, and stress.[3–5]

Because IVD degeneration is an irreversible progressive disease, various treatments are currently being developed to repair and regenerate damaged IVDs. Experimental regenerative medicine techniques for IVD degeneration include the intradiscal injection of cytokines and growth factors,[6–10] gene delivery to IVD cells,[11–13] creation of artificial IVDs using tissue engineering,[14] and cell transplantation.[15–18] In vitro and in vivo studies using these techniques have reported increased IVD cell activity, the stimulation of extracellular matrix synthesis, and the suppression of IVD degeneration.

Recent advances in molecular biology and regenerative medicine have drawn an attention to mesenchymal stem cells (MSCs), because these immature cells remain pluripotent, capable of differentiating into bone, cartilage, or fat cells depending on their treatment. Undifferentiated MSCs are also immune tolerant. Autologous MSC transplantation has become an important treatment for various diseases.[19,20] Facilitating clinical applications, MSCs are easily harvested, and extracorporeal isolation and culture are relatively simple, requiring no highly specialized procedures. A number of basic studies have been performed using MSC transplantation into IVDs. Sakai et al.[15] performed autologous MSC transplantation using a rabbit IVD degeneration model, showing by radiology, histology, and biochemistry that this procedure suppressed IVD degeneration. They also analyzed the differentiation of transplanted MSCs into nucleus pulposus cells, establishing that transplanted MSCs expressed markers for the resident nucleus pulposus cells, indicating that the differentiation of MSCs is dependent on their environment.[16,17] Hiyama et al.[18] examined the immune privilege of IVD tissue, particularly the nucleus pulposus, including the anatomical characteristics separating disc tissue from the host immune system. Using a canine IVD degeneration model, these authors transplanted MSCs and measured changes in the expression of the Fas/Fas-ligand (FasL) system in addition to ascertaining any suppressive effects of the transplant on disc degeneration. In their study, the transplantation of MSCs suppressed IVD degeneration as assessed by radiological, histological, and biochemical findings. Their results also suggest that MSC transplantation could be effective in maintaining the immune privilege of IVDs.

Based on these studies and others, MSC transplantation into degenerated IVDs offers a promising new interventional technique in animal models.[21,22] Although the efficacy of MSC transplantation has been documented, some questions remain unanswered. For

Correspondence to: Daisuke Sakai (T: 81-463-93-1121 ext. 2320; F: 81-463-96-4404; E-mail: daisakai@is.icc.u-tokai.ac.jp)